NASA TECHNICAL NOTE

NASA TN D-3219

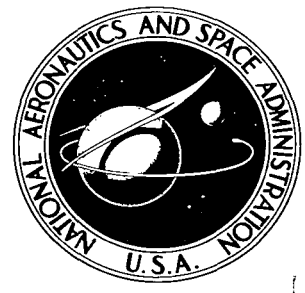

NASA TN D-3219

EXPERIMENTAL AND ANALYTICAL INVESTIGATION OF INTERFACIAL HEAT AND MASS TRANSFER IN A PRESSURIZED TANK CONTAINING LIQUID HYDROGEN

by William A. Olsen

Lewis Research Center
Cleveland, Ohio

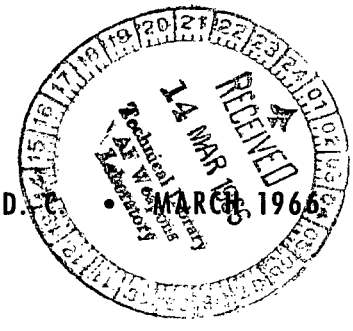

NATIONAL AERONAUTICS AND SPACE ADMINISTRATION • WASHINGTON, D.C. • MARCH 1966

NASA TN D-3219

EXPERIMENTAL AND ANALYTICAL INVESTIGATION OF INTERFACIAL HEAT AND MASS TRANSFER IN A PRESSURIZED TANK CONTAINING LIQUID HYDROGEN

By William A. Olsen

Lewis Research Center
Cleveland, Ohio

NATIONAL AERONAUTICS AND SPACE ADMINISTRATION

For sale by the Clearinghouse for Federal Scientific and Technical Information
Springfield, Virginia 22151 – Price $2.00

EXPERIMENTAL AND ANALYTICAL INVESTIGATION OF INTERFACIAL HEAT AND MASS TRANSFER IN A PRESSURIZED TANK CONTAINING LIQUID HYDROGEN

by William A. Olsen

Lewis Research Center

SUMMARY

Temperature measurements in the vicinity of the placid interface of two-phase hydrogen contained in a pressurized tank have yielded information on interfacial heat and mass transfer. These measurements indicated that interfacial mass transfer can have an appreciable effect on bulk gas and liquid conditions, while heat transfer from the gas can probably be neglected in most cases. An analysis of interfacial heat and mass transfer, which closely predicts the data, is included herein.

INTRODUCTION

Cryogenic propellant tanks are pressurized to cause outflow, prevent pump cavitation, and/or stiffen the structure of the tank. When a tank is suddenly pressurized (artificial pressurization) to a new level from an initial equilibrium state, the two-phase fluid system attempts to go to a new equilibrium situation at the higher pressure by the transfer of heat across the tank walls from the environment, and heat and mass transfer across the interface. Heat transfer from the environment heats liquid at the tank walls, which then flows up the walls and forms a growing layer of relatively warm liquid below the interface. Heat and mass transfer across the interface tends to enlarge this warm layer of liquid. Similar energy and mass transfer occur while the liquid is expelled from the tank or the tank pressure builds up slowly as a result of the heat leak (self-pressurization).

There have been several analytical and/or experimental studies that have examined this complex nonequilibrium process (refs. 1 to 10). However, none of these studies experimentally investigated the interfacial region and interfacial heat and mass transfer in detail.

In references 1 and 2, analytical and experimental studies of pressurization were performed. The former used an overall heat and mass balance that yielded only rough estimates of interfacial heat and mass transfer. References 3 and 4 were concerned with stratification in high-heat-flux tanks but did not consider interfacial transfers. In reference 5 the effect of interfacial transfers on tank pressure was experimentally observed when the bulk liquid or gas was artificially mixed. Similar analyses of interfacial heat and mass transfer were performed in references 6 to 8. In reference 9, pressurization and stratification were studied analytically considering interfacial transfers. Probably the most applicable experimental study of interfacial transfer is given in reference 10, which obtained detailed experimental temperature profile data $T = T\langle Z, t\rangle$ for a very low-heat-flux self-pressurized tank. (All symbols are defined in the appendix.) Only a very limited evaluation of interfacial heat and mass transfer was performed.

As part of a general study at the Lewis Research Center of internal fluid conditions in pressurized propellant tanks containing cryogens, the interfacial region was experimentally studied more extensively than in previous references to determine the interfacial heat and mass transfer for artificially and self-pressurized tanks where the heat flux was not small. In addition, the results of this experimental study were compared with corresponding results of the now standard analytical method to predict heat and mass transfer in suddenly pressurized tanks.

ANALYSIS OF INTERFACIAL HEAT AND MASS TRANSFER

Physical Description of Problem

When a vented tank containing a two-phase one-component cryogenic fluid in equilibrium is rapidly pressurized to a new constant pressure by adding gas, the system tends toward a new equilibrium condition at that new pressure (fig. 1). Gas near the interface is rapidly compressed by the well-diffused (little mixing) incoming gas. Gas near the interface, which was heated by compression, begins to cool by heat transfer to the liquid. The interface immediately assumes the new equilibrium state (saturation). (Kinetic theory requires some difference between the interface temperature and saturation; however, this difference is generally small for a pure fluid, refs. 6 to 8.) Concurrently, the liquid begins to be heated by heat and mass transfer from the warm gas and heat transfer from the environment.

All the heat transferred to the liquid will be stored nonuniformly in the liquid, resulting in stratification (i. e., temperature gradients, $T = T\langle Z, t\rangle$). The environmental heat flux through the side walls of the tank to the liquid causes relatively warmer liquid to flow up the tank and form a warm layer near the interface (fig. 1), which is further

heated by interfacial heat and mass transfer. Heat transferred across the tank bottom from the environment will essentially heat up the bulk liquid below this warm layer of liquid (ref. 11).

Analysis of Artificial Pressurization

Except for the specification of some of the boundary conditions, the analysis of this problem has been performed many times (refs. 6 to 8). The analysis used in reference 6, which is most easily used here, is summarized subsequently only for the reader's convenience. Basically these analyses assume that the flows and heat transfer occurring in the region of the interface of the complex system previously described can be physically approximated by two semi-infinite volumes of gas and liquid joined by an interface (fig. 2). Using a moving coordinate system, attached to the interface, gives the differential equations and boundary conditions describing conditions in the gas and liquid near the interface as

$$\frac{\partial T_g}{\partial t} + W_g \frac{\partial T_g}{\partial Z} = \alpha_g \frac{\partial^2 T_g}{\partial Z^2} \tag{1}$$

$$\frac{\partial T_\ell}{\partial t} + W_\ell \frac{\partial T_\ell}{\partial Z} = \alpha_\ell \frac{\partial^2 T_\ell}{\partial Z^2} \tag{2}$$

The boundary conditions are (fig. 2):

$$t < 0,\ Z = Z:\ T_\ell = T_g = T_o \tag{3), (4}$$

$$t \geq 0: \begin{cases} Z = +\infty:\ T_\ell = T_b & (5) \\ Z = -\infty:\ T_g = T_r & (6) \\ Z = 0:\ T_g = T_\ell = T_i & (7), (8) \end{cases}$$

where T_o, T_b, T_r, and T_i are not functions of time or position.

The velocities W_g and W_ℓ are obtained by an interfacial mass balance and an

interfacial energy balance. The interfacial mass balance, which satisfies the continuity equation is

$$\rho_g W_g = \rho_\ell W_\ell = \left(\frac{\dot{m}}{A}\right)_i \tag{9}$$

The interfacial energy balance is

$$-\left(k_g \frac{\partial T_g}{\partial Z}\right)_{Z=0} + \left(k_\ell \frac{\partial T_\ell}{\partial Z}\right)_{Z=0} + \rho_g W_g L = 0 \tag{10}$$

The partial differential equations (eqs. (1) and (2)) are transformed to ordinary differential equations by the following substitutions (refs. 6 to 8)

$$\theta_j \equiv \frac{c_{p_j}(T_j - T_i)}{L} \tag{11}$$

$$V_j \equiv W_j \left(\frac{t}{\alpha_j}\right)^{1/2} \tag{12}$$

and the similarity substitution

$$\eta_j \equiv \frac{Z}{\left(4\alpha_j t\right)^{1/2}} \tag{13}$$

where j denotes gas or liquid. These substitutions (eqs. (11) to (13)) convert the partial differential equations (1) and (2) to ordinary differential equations:

$$\frac{d^2\theta_g}{d\eta_g^2} = -\frac{2d\theta_g}{d\eta_g}(\eta_g - V_g) \tag{14}$$

$$\frac{d^2\theta_\ell}{d\eta_\ell^2} = -\frac{2d\theta_\ell}{d\eta_\ell}(\eta_\ell - V_\ell) \tag{15}$$

The resulting transformed boundary conditions become:

$$\eta_\ell = +\infty: \quad \theta_\ell = \theta_b \tag{16}$$

$$\eta_g = -\infty: \quad \theta_g = \theta_r \tag{17}$$

$$\eta_\ell = \eta_g = 0: \quad \theta_\ell = \theta_g = 0 \tag{18), (19}$$

The interfacial energy and mass balances are transformed by equations (11) to (13) to

$$\rho_\ell(\alpha_\ell)^{1/2}V_\ell = \rho_g(\alpha_g)^{1/2}V_g \tag{20}$$

$$\left[\rho_\ell(\alpha_\ell)^{1/2}\frac{d\theta_\ell}{d\eta_\ell}\right]_{\eta_\ell=0} - \left[\rho_g(\alpha_g)^{1/2}\frac{d\theta_g}{d\eta_g}\right]_{\eta_g=0} = -2(\alpha_g)^{1/2}\rho_g V_g \tag{21}$$

Solutions of the differential equations (eqs. (14) and (15)) are given subsequently. The solutions describe the temperature profiles in the gas and liquid in the vicinity of the interface:

$$\theta_g = \theta_r\left[\frac{\text{erf}(V_g) - \text{erf}(V_g - \eta_g)}{\text{erf}(V_g) - 1}\right] \tag{22}$$

$$\theta_\ell = \theta_b\left[\frac{\text{erf}(V_\ell) - \text{erf}(V_\ell - \eta_\ell)}{\text{erf}(V_\ell) + 1}\right] \tag{23}$$

Interfacial mass transfer is obtained from equations (9) and (12):

$$\left(\frac{\dot{m}}{A}\right)_i = \rho_g V_g\left(\frac{\alpha_g}{t}\right)^{1/2} \tag{24}$$

Interfacial heat transfer to the liquid is obtained from equations (11), (13), and (23) according to

$$\left(\frac{q_\ell}{A}\right)_i = -\left(k_\ell \frac{\partial T_\ell}{\partial Z}\right)_i \tag{25}$$

to achieve

$$\left(\frac{q_\ell}{A}\right)_i = -\left(\frac{2}{\pi^{1/2}}\right)\frac{\exp\left(-V_\ell^2\right)k_\ell L\theta_b}{\left[\operatorname{erf}(V_\ell) + 1\right]c_{p_\ell}(4\alpha_\ell t)^{1/2}} \tag{26}$$

Interfacial heat transfer from the gas is obtained from equations (11), (13), and (22) according to

$$\left(\frac{q_g}{A}\right)_i = -\left(k_g \frac{\partial T_g}{\partial Z}\right)_i \tag{27}$$

to obtain

$$\left(\frac{q_g}{A}\right)_i = -\left(\frac{2}{\pi^{1/2}}\right)\frac{\exp\left(-V_g^2\right)k_g L\theta_r}{\left[\operatorname{erf}(V_g) - 1\right]c_{p_g}(4\alpha_g t)^{1/2}} \tag{28}$$

The nondimensional velocities V_g and V_ℓ required in equations (24), (26), and (28) are obtained from the simultaneous solution of

$$-\pi^{1/2} = \frac{\theta_b}{\left\{V_\ell\left[\exp\left(V_\ell^2\right)\right]\right\}\left[1 + \operatorname{erf}(V_\ell)\right]} - \frac{\theta_r}{\left\{V_g\left[\exp\left(V_g^2\right)\right]\right\}\left[\operatorname{erf}(V_g) - 1\right]} \tag{29}$$

and

$$\rho_\ell(\alpha_\ell)^{1/2}V_\ell = \rho_g(\alpha_g)^{1/2}V_g \tag{20}$$

Equation (29) was obtained by differentiating equations (22) and (23) and substituting into equation (21).

Values of the constant thermal boundary conditions (eqs. (5) to (8)) will now be specified based on the physics of the problem. The interface temperature T_i should be very nearly the saturation temperature $T_i \simeq T_{sat}$, which will be constant after the tank has been rapidly pressurized to a constant pressure. The interface is assumed to offer no resistance to mass transfer (refs. 8 and 12).

The initial gas is assumed to be rapidly compressed by the incoming gas with no mixing, and thereafter the heat transfer is small so that the changes in T_r are small. A reasonable choice for T_r, therefore, appears to be the adiabatic compression temperature of the gas, which will be constant. Thus T_r is assumed to be

$$T_r \simeq T_{ad} = T_o\left(\frac{P}{P_o}\right)^{\frac{\gamma-1}{\gamma}} \tag{30}$$

where $\gamma \simeq 1.8$ for gaseous hydrogen for $37^o\ R < T_r < 50^o\ R$. The bulk liquid boundary condition T_b is obtained by assuming that the change in the liquid temperature through the heat leak is small enough so that T_b can be taken as the initial temperature T_o. Thus, $T_b \simeq T_o$.

In summary, the values for the boundary conditions are considered to be

$$T_i = T_{sat} = T_{sat\langle P\rangle} \tag{31}$$

$$T_r = T_{ad} = T_{ad\langle P\rangle} = T_o\left(\frac{P}{P_o}\right)^{\frac{\gamma-1}{\gamma}} \tag{32}$$

$$T_b = T_o \tag{33}$$

and the properties can be evaluated at $T_i = T_{sat\langle P\rangle}$ since the analysis only holds near the interface.

APPARATUS AND PROCEDURE

General Description of Experiment

The experiment can be described as a tank containing a two-phase fluid initially at a uniform temperature and low pressure that is suddenly raised to a higher pressure. The pressure is either increased quickly by the addition of gaseous hydrogen or helium (artificial pressurization) or slowly by heat leak (self-pressurization). Fluid temperatures, tank pressure, and liquid level data are recorded as the fluid tends toward a new equilibrium state. Tank pressure, pressurant gas, and method of pressurization are varied as parameters (see table I).

Description of Test Facility

The test facility consisted of a large vacuum-jacketed tank (30 in. in diam. by 88 in. long, fig. 3(a)) that could be filled, emptied, and pressurized automatically. A 3-foot-long carbon-resistor temperature rake was vertically fastened to the lid so that it was at the center of the tank. A viewing window, allowed the experimenter to observe the fluid conditions in the tank. The tank could be pressurized up to 40 pounds per square inch gage.

Description of Temperature Rake

The 3-foot-long vertical temperature rake used in this study consisted of forty-two 0.07-inch-diameter 1/10 watt calibrated carbon resistors, which were fastened to a Bakelite superstructure at various levels (fig. 3). Thirteen resistors, which supplied the significant interfacial data, were spaced 1/4 inch apart at the middle of the rake (fig. 3). An effort was made to keep the carbon resistors isolated from significant thermal and hydrodynamic error sources by means of low conductivity supports and lead wires (manganin alloy) and a tree-like rake structure that did not disturb the flow significantly.

Procedure

Two types of tests were performed. One was artificial pressurization, where gas at about room temperature is forced through a diffuser into a tank to bring the tank to some higher pressure, which is then held constant (tests 1 to 3). The diffuser was de-

signed so that it caused very little gas mixing. The other type of test was self-pressurization, where the vent valve is closed and the tank pressure would build up by heat leak (test 4).

Artificial pressurization (tests 1 to 3). - The liquid level was initially visually set at about the middle of the 1/4 inch spaced resistors on the temperature rake. The initially vented tank was then quickly pressurized with the desired gas to a preset pressure, which was thereafter held constant. About 1 minute was required to attain the desired pressure. At specific time intervals after the start of pressurization, the temperature profile and tank pressure were recorded by automatic self-balancing digital recording equipment. After completion of a test, the tank pressure and/or pressurant gas were then changed, and the preceding procedure was repeated. Throughout each test the liquid condition was visually monitored. The heat flux was measured for a given liquid depth and vacuum pressure by noting the boiloff before and after each run.

Self-pressurization. - The only difference between the self-pressurization and the artifical pressurization tests was that the vent valve was closed to build up pressure slowly by heat leak in the former whereas pressurant gas was added in the latter to attain a constant pressure.

Instrumentation Accuracy

The position of the carbon resistors with respect to one another was known to within 0.05 inch including thermal dimension changes. The entire temperature rake was immersed in boiling liquid hydrogen (at atmospheric pressure) before each test run to check its thermal accuracy at a known condition. Temperature errors due to thermal conduction through the leads and the rake, thermal radiation from the tank walls and lid, and electrical heating in the carbon resistors were estimated analytically. Based on these estimates and the temperature check in boiling hydrogen, it is expected that a thermal error of no greater than $\pm 0.1^{\circ}$ R will result. The thermal time lag (time constant) of the carbon resistor thermometers in liquid and gaseous hydrogen (maximum temperature difference $\lesssim 200^{\circ}$ R) was analytically estimated to be less than 0.2 and 2 seconds, respectively. This lag results in a negligible thermal error for this slow transient experiment.

The automatic system that controlled the tank pressure maintained a fairly constant pressure that varied no more than ±5 percent around the nominal pressures listed in table I. Tank pressure was sensed within ±0.1 percent of full scale, which would result in an error in the saturation temperature no greater than $\pm 0.05^{\circ}$ R.

The overall heat flux (based on the liquid-wetted area) for a given liquid depth and vacuum jacket pressure was determined by measuring the rate at which liquid was

boiled off when the tank was vented to the atmosphere ($P' = 0$ psig). From this information the heat flux could be approximately calculated by using equation (34):

$$\left(\frac{Q}{A}\right)_w \simeq \left(\frac{LA_i\rho_\ell}{A_w}\right)\frac{dh}{dt} \tag{34}$$

Because of greater possible changes in the liquid temperatures at the higher tank pressure levels, it is recognized that the experimentally determined heat-leak values will be in excess of the actual quantities (i.e., $(Q/A)_w$ is proportional to $T_\infty - T_\ell$). Within the limits of the tests conducted, however, this error should not exceed 2 percent.

DATA PROCESSING

The interface location is determined from temperature profile data ($T = T\langle h, t\rangle$) by assuming that the interface is saturated. This assumption was also made in the analyses and in other references (e.g., refs. 1, 6 to 8, and 10). From the level location and temperature profile data, interfacial data can be obtained. For example, the interfacial heat transfer from the gas is obtained from equation (25) where $(q_g/A)_{int} = -(q_g/A)_i$ and $\partial T_g/\partial Z = -(\partial T_g/\partial h)$ to give

$$\left(\frac{q_g}{A}\right)_{int} = -\left(k_g\frac{\partial T_g}{\partial h}\right)_{int} \tag{35}$$

The interfacial heat transfer to the liquid is similarly obtained from equation (27) to give

$$\left(\frac{q_\ell}{A}\right)_{int} = -\left(k_\ell\frac{\partial T_\ell}{\partial h}\right)_{int} \tag{36}$$

The mass flux transferred across the interface for a given time can be obtained experimentally from the one-dimensional energy balance described by equation (10) where

$$\left(\frac{\partial T}{\partial Z}\right)_{int} = -\left(\frac{\partial T}{\partial h}\right)_{int}$$

and

$$\rho_g W_g = -\left(\frac{\dot{m}}{A}\right)_{int}$$

It is assumed that

$$\left(\frac{\partial T_g}{\partial h}\right)_{int} \equiv \left(\frac{\partial T_\ell}{\partial h}\right)_{int}$$

which gives

$$\left(\frac{\dot{m}}{A}\right)_{int} = -\frac{1}{L}\left[(k_\ell - k_g)\frac{\partial T_\ell}{\partial h}\right]_{int} \tag{37}$$

Two further assumptions are inherent in equations (35) to (37). Radial temperature gradients in the gas and liquid in the vicinity of the interface (when the region near the tank walls is excluded from consideration entirely) were assumed to be negligible. Radial temperature profiles near the interface have been measured in pressurized outflow studies (unpublished data obtained by R. DeWitt of Lewis). These data indicate that the assumption is reasonable. The second assumption is that the significant temperature gradients occur over a sufficient distance so that a finite number of thermometers (carbon resistors spaced 1/4 in. apart) would be able to detect and to measure these gradients.

RESULTS AND DISCUSSION

Vertical temperature profiles in the liquid and gas and tank pressures were taken at various time intervals after the start of pressurization. The method of pressurization, pressurant gas, and pressure level were varied (see table I).

Artificial Pressurization with Hydrogen Gas Tests - 1 and 2

Raw data. - In the interest of brevity, only one typical group of rake-length temperature profiles ($T = T\langle h, t, P'\rangle$) will be reported. Figure 4 contains the profiles for test 1 at a tank pressure of 40 pounds per square inch gage. The portion of this profile where the temperature sensors are spaced at 1/4-inch intervals (i. e., the region about 1. 5 in.

on either side of the interface) is enlarged in figure 5(c). Figures 5(a) and (b) contain this type of data for tank pressures of 8 and 20 pounds per square inch gage. Figure 6 contains a similar enlargement for test 2 data. The solid lines represent the author's judgement of the best fairing. The saturation-dictated interface location is also plotted in each of these figures.

Interfacial heat and mass transfer. - Interfacial mass transfer, as obtained from the analysis[1] (eqs. (20), (24), and (29)), is plotted in figure 7. The experimental interfacial mass fluxes that occurred during tests 1 and 2 are determined from the temperature profiles (figs. 5 and 6) at the saturation-dictated interface according to equation (37). These data are also plotted for comparison in figure 7. Agreement between the analysis and the experimental data is generally good. Figure 7 indicates that the mass transfer is condensation which increases with tank pressure and decreases with time.

The analytically determined interfacial heat transfer to the liquid (eqs. (20), (21), and (26)) is plotted in figure 8. Also shown are experimental values of heat transfer to the liquid as determined from equation (36). These results also indicate good agreement between the analysis and the experiment. Again, interfacial heat transfer to the liquid increases with pressure and decreases with time.

Figure 9 contains the analytical (eqs. (20), (21), and (28)), and experimentally (eq. (35)) determined values for interfacial heat transfer from the gas when it is assumed that there is no discontinuity in the slope at the interface [i.e., $(\partial T_g/\partial Z)_i \equiv (\partial T_\ell/\partial Z)_i$.] Agreement between the analysis and the experiment is poor especially for increasing tank pressure. Fortunately, heat transfer from the gas is small compared with heat transfer to the liquid so that mass transfer is not greatly affected by this error. This can be seen from equation (37) where $k_\ell >> k_g$. The reasons for this disagreement are discussed in the section titled Interfacial boundary conditions.

Artificial Pressurization with Helium - Test 3

In a two-component two-phase system, interfacial heat and mass transfer caused by temperature differences and component mass transfer (diffusion) caused primarily by concentration differences are coupled. Consequently, it should be expected that experimental measurements would be complex. Because of the scarcity of diffusion-coefficient data and the difficulty in sampling the concentration of components in a transient system, only significant raw data from the helium pressurant test (test 3) will be reported. The

[1]A copy of the analytical computer program, written by Margaret M. Smith, can be obtained from Instrument and Computing Division, Lewis Research Center.

temperature profiles near the interface are plotted in figure 10.

In general, the effective saturation temperature of this two-component system (hydrogen-helium pressurant) $T_{sat}*$ should not be the same as the saturation temperature for the one-component system (hydrogen, tests 1 and 2) T_{sat}. As a rough indication of the interface location in figure 10, it was assumed that $T_{sat} \simeq T_{sat}*$; however, no more can be done with this data because of the lack of concentration data.

Self-Pressurization - Test 4

With the vent valve closed, the tank pressure rose from $P'_o = 0$ pounds per square inch gage at a uniform rate of 0.4 pound per square inch gage per minute as a result of the heat leak. Figure 11 is a plot of the temperature profiles in the vicinity of the interface for this test. A comparison of heat and mass flux data between artificial and self-pressurization tests reveal different trends; in this test, both quantities increased with time. Some slight boiling was noted at the tank walls near the interface during most of the test. Excluding the mass transferred by this boiling at the walls, heat and mass transfer was calculated by equations (35) to (37) and plotted in figure 12. These fluxes are much smaller than those for artificial pressurization. The analysis is not applicable for this case where the saturation temperature varies with time because of the time-varying pressure, therefore no effort was made to correlate these data with the analysis.

Discussion of Boundary Conditions

The boundary conditions were specified on the basis of physical arguments. The object of this section is to discuss and justify, by means of analysis and experiment, the values of T_r and T_b and the interfacial boundary conditions.

Bulk fluid boundary conditions. - The bulk liquid temperature, which was assumed to be constant (i.e., $T_b = T_o$) in the analysis, will actually increase slowly with time because of the heat leak from the environment to the liquid. If it is assumed that all the heat leak from the environment is stored uniformly in the bulk liquid, T_b can be approximated by

$$T_b = T_{b\langle t\rangle} \simeq T_o + \frac{\left(\frac{Q}{A}\right)_w}{\rho_\ell c_{p_\ell} D}\left(\frac{D}{H_\ell} + 4\right)\frac{t}{3600} = T_o + K\left(\frac{D}{H_\ell} + 4\right)t \qquad (38)$$

This function (eq. (38)) is approximated by a series of finite steps and is used in the analysis to give an estimate of the effect of this time-varying boundary condition on interfacial mass transfer. The result of this calculation is plotted in figure 13 for pressures of 20 and 100 pounds per square inch gage and various values of $K\left[K = (Q/A)_w/3600\rho_\ell c_{p_\ell} D\right]$ and H_ℓ/D. The two single-line curves, 5 and 1 are for tanks with zero environmental heat flux (K = 0). The band curves 2 to 4 and 6 to 8 describe the range of mass fluxes for $2 > H_\ell/D > 0.5$ that occur for various heat fluxes. The upper part of the band corresponds to an H_ℓ/D of 2 and the lower part to an H_ℓ/D of 0.5.

Figure 13 indicates that the effect of environmental heat leak on interfacial mass transfer is to decrease the mass flux to a lower value than would be predicted by a constant value of $T_b (T_b = T_o)$. Compare curve 5 to 6 and 7, or compare 1 to 2 and 3 in figure 13. This difference increases with time. The effect on interfacial mass transfer by changes in T_b caused by heat leak is small for $t < 10$ minutes and $K < 7\times10^{-4}$ ^oR per second, or $t < 30$ minutes and $K < 7\times10^{-5}$ (fig. 13). The former situation would correspond to a heat flux of 85 Btu per square foot per hour for a 3-foot-diameter tank or about 280 Btu per square foot per hour for a 10-foot-diameter tank. The "centerline" of the band of curve 2 corresponds to the experimental situation of tests 1 and 2 where the heat flux was about 8 Btu per square foot per hour. It appears that interfacial mass transfer can be predicted approximately by using the constant liquid boundary condition $(T_b = T_o)$ for most practical situations (where $K = (Q/A)_w/3600\rho_\ell c_{p_\ell} D < 7\times10^{-4}$ ^oR/sec and the time is small).

Some justification is required for the choice of the bulk gas thermal boundary condition T_r chosen in the analysis. Both the analysis and experiment were based on situations where the gas volume is not appreciably mixed by the rapid introduction of pressurizing gas. In this situation, one might expect the pressurizing gas to compress the original gas adiabatically during a rapid pressurization. The main justification for the choice of the boundary condition $T_r = T_{ad}$ is that the interfacial heat transfer to the liquid and mass transfer predicted by the analysis closely agrees with the experiment. On the negative side there is poor agreement in interfacial heat transfer from the gas. This disagreement is discussed further in the next section.

Interfacial boundary conditions. - Based on the usual thermodynamic assumption of local equilibrium, the following are the accepted theoretical interfacial boundary conditions (ref. 13):

$$T_{g,i} = T_{\ell,i} = T_{sat} \tag{7}$$

$$-\left(k_g \frac{\partial T_g}{\partial Z}\right) + \left(k_\ell \frac{\partial T_\ell}{\partial Z}\right) + \rho_g W_g L = 0 \qquad (10)$$

References 6 to 8 made use of these two equations in their analysis, and they have been used in this report in order to evaluate the data. The first equation (eq. (7)) is considered approximate and should be experimentally verified. Considering the temperature profile data it seems reasonable that $\left(\partial T_g/\partial Z\right)_i \sim \left(\partial T_\ell/\partial Z\right)_i$, and since k_ℓ is about an order of magnitude greater than k_g, it is reasonable to state that heat transfer from the gas (first term in eq. (10)) has little effect on mass transfer (third term) or on heat transfer to the liquid (second term). Therefore it should be expected that the data analysis, which assumed $\left(\partial T_g/\partial Z\right)_i \equiv \left(\partial T_\ell/\partial Z\right)_i$, should give good results for interfacial mass transfer and heat transfer to the liquid, but poor results for interfacial heat transfer from the gas. This was indeed shown to be the case in figures 7 to 9. The analysis indicates that $\left(\partial T_g/\partial Z\right)_i \equiv \left(\partial T_\ell/\partial Z\right)_i$ is not a good assumption. Figure 14 is a plot of the analytically determined ratio of the liquid and gas temperature gradients at the saturation-dictated interface $\left(\partial T_g/\partial Z\right)_i / \left(\partial T_\ell/\partial Z\right)_i$. Such small discontinuities could not have been observed in this experiment if they had existed, because the sensors are 0.07 inch in diameter and 1/4 inch apart. Examples of such local slope discontinuities are plotted in figure 5.

Effect of Interfacial Heat and Mass Transfer on Bulk Fluid Conditions

Although the flow of condensate appears to be small (fig. 7), its effect on conditions in the bulk gas and liquid may not be small in the artificially pressurized case. For example, consider a gas space (ullage) H_g feet high that is quickly pressurized by gaseous hydrogen to a constant pressure of 60 pounds per square inch gage. With the gas temperature held constant at 300° R, the fraction of the total mass of gas that will condense and must be replaced in order to hold a constant pressure during the first 5 minutes after the start of pressurization is given as follows (based on fig. 7):

$$\frac{\text{Mass condensed}}{\text{Total mass of gas}} = \frac{\overline{\left(\frac{\dot{m}}{A}\right)_i} \Delta t}{\rho_g H_g} \simeq \frac{0.17 \frac{5}{60}}{0.047 H_g}$$

For ullage heights H_g of 0.5, 1, and 5 feet, the fraction of the total mass that will condense is 60, 30, and 6 percent, respectively. This estimate indicates that the effect of

condensation of the gas should be considered in bulk gas problems such as pressurized outflow.

The effect of interfacial heat transfer from the gas on the bulk gas conditions is now considered. For the worst situation described in the preceding paragraph, the interfacial heat transfer from the gas as a fraction of the total enthalpy of the gas, based on the analytical data of figure 9 is:

$$\frac{\text{Interfacial heat flux from gas}}{\text{Total enthalpy of gas}} = \frac{\left(\frac{\overline{q_g}}{A}\right)_i \Delta t}{\rho_g \dot{w}_g H_g}$$

$$\simeq \frac{18\,\frac{5}{60}}{0.047 \times 1020 \times 0.5}$$

$$\simeq 0.06 \text{ or } 6 \text{ percent}$$

This conservative estimate indicated that the effect of interfacial heat transfer from the gas on the bulk conditions of the gas is small enough to neglect in most bulk gas problems and makes the inability of the analysis to predict it of lesser consequence.

A representative high heat flux from the environment for booster vehicles is about 50 Btu per square foot per hour. According to figure 8, interfacial heat transfer to the liquid is not generally small compared with this figure, so that it should generally be considered in bulk liquid heating analyses.

Effect of Bulk Fluid Mixing on Hydrogen

The bulk gas temperature used in the analysis T_{ad} was for a situation where there was little gas mixing. It could conceivably be quite different if there were sufficient gas mixing, caused by a poorly distributing diffuser, to raise T_r above T_{ad}. Consequently, constant values of T_r greater than T_{ad} were used in the analysis to investigate their effect on interfacial mass transfer. The result of this study is shown in figure 15. As T_r increases, there is a tendency toward evaporation, away from the condensation result that occurs when the adiabatic temperature is used. With the proper choice of boundary conditions, no net mass transfer is possible. For the case of no net mass transfer (refs. 6 to 8) equations (20) and (29) reduce to

$$\frac{T_r - T_{sat}}{T_{sat} - T_b} = -\frac{\rho_\ell}{\rho_g}\left(\frac{\alpha_\ell}{\alpha_g}\right)^{1/2}\frac{c_{p_\ell}}{c_{p_g}} \tag{39}$$

This result for zero net mass transfer, which is a function of the fluid properties alone (or since the properties are evaluated at T_{sat}, a function of pressure for a given fluid), is plotted in figure 16 to indicate regions of evaporation and condensation.

The experiment of reference 5 is described here to show that mixing is attainable and can have an appreciable effect on interfacial transfer. The results of this experiment will be qualitatively compared with figure 16. Stirrers were placed in the liquid and gas volumes, near the interface, of a closed Dewar containing two-phase nitrogen. These stirrers were used to mix either the liquid or gas volumes in order to determine the effect of mixing on the tank pressure. It was observed that the pressure rose when the gas was mixed and that the tank pressure dropped when the liquid was mixed. Qualitatively, this mixing raises the gas temperature near the interface T_r by mixing cool gas near the interface with warm gas above it, and lowers the liquid temperature T_b by mixing cool liquid of the bulk with warm liquid near the interface. Consider figure 16, which is the locus of pressure-temperature conditions for zero mass transfer for a hydrogen system; a similar curve can be generated for nitrogen. Qualitatively, according to figure 16, an increase in T_r by mixing the gas would tend to cause evaporation and raise the tank pressure, while a decrease in T_b by liquid mixing would tend to cause condensation and lower the tank pressure.

It was shown before that condensation could be a major detrimental effect in that it increases the mass of pressurant required and heats the liquid. Evaporation at the interface would be more desirable since it would tend to cool the liquid and decrease pressurization requirements. According to the previous discussion it can be implied that evaporation or at least a lower condensation rate can be achieved by mixing the gas by some method that does not also mix the liquid.

CONCLUDING REMARKS

The condensation that occurs in a tank containing two-phase hydrogen that is rapidly pressurized without mixing creates an appreciable transfer of heat to the liquid which must be considered in stratification studies. The analysis included herein can be used to determine the interfacial heat transfer. The effect, on pressurization requirements, of interfacial heat transfer can probably be neglected, while the effect of interfacial mass

transfer (condensation) should be considered. Interfacial mass transfer can be determined by the analysis contained in this report.

Lewis Research Center,
National Aeronautics and Space Administration,
Cleveland, Ohio, October 20, 1965.

APPENDIX - SYMBOLS

A	area, sq ft
c_p	specific heat at constant pressure, Btu/(lb mass)(^oR)
D	tank diameter, ft
H	height, ft
$\mathfrak{h}$	specific enthalpy, Btu/lb mass
h	liquid depth (height above average tank bottom), ft
K	$(Q/A)_w/3600\rho_\ell c_{p_\ell} D$, ^oR/sec
k	thermal conductivity, Btu/(ft)(^oR) or Btu/(ft)(^oR)(sec)
L	heat of vaporization, Btu/lb mass
$\dot{m}/A$	interfacial mass flux, lb mass/(sq ft)(sec)
P	tank pressure, psfa
P'	tank pressure (gage), psig
$(Q/A)_w$	heat flux through tank walls from environment, Btu/(sq ft)(hr)
(q_g/A)	interfacial heat flux from gas, Btu/(sq ft)(sec)
(q_ℓ/A)	interfacial heat flux to liquid, Btu/(sq ft)(sec)
T	temperature, ^oR
t	time (after pressurization), sec
V_j	nondimensional velocity, $\equiv W_j(t/\alpha_j)^{1/2}$
W	flow velocity in Z-direction relative to moving interface, ft/sec
Z	distance below the interface, ft
α	thermal diffusivity, sq ft/sec
γ	ratio of specific heats
η_j	dimensionless similarity variable, $\equiv Z/(4\alpha_j t)^{1/2}$
θ_j	dimensionless temperature, $\equiv \dfrac{c_{p_j}(T_j - T_i)}{L}$
ρ	density, lb mass/cu ft

Subscripts:

ad	adiabatic
b	bulk liquid
g	gas
f	final
int	saturation interface in coordinate system in h
i	saturation interface in movable coordinate system in Z
j	gas or liquid
ℓ	liquid
o	initial
r	bulk gas
sat	saturation
sat*	helium-hydrogen effective saturation temperature assumed to be that of pure hydrogen
w	wetted wall
∞	environment outside tank

REFERENCES

1. Gluck, D. F.; and Kline, J. F.: Gas Requirements in Pressurized Transfer of Liquid Hydrogen. Vol. 7 of Advances in Cryogenic Eng., K. D. Timmerhaus, ed., Plenum Press, 1961, pp. 219-233.

2. Arpaci, V. S.; Clark, J. A.; and Winer, W. D.: Dynamic Response of Fluid and Wall Temperatures During Pressurized Discharge of a Liquid from a Container. Vol. 6 of Advances in Cryogenic Eng., K. D. Timmerhaus, ed., Plenum Press, 1961, pp. 310-322.

3. Bailey, T. E.; and Fearn, R. F.: Analytical and Experimental Determination of Liquid-Hydrogen Temperature Stratification. Vol. 9 of Advances in Cryogenic Eng., K. D. Timmerhaus, ed., Plenum Press, 1964, pp. 254-264.

4. Tatom, J. W.; Brown, W. H.; Knight, L. H.; and Coxe, E. F.: Analysis of Thermal Stratification of Liquid Hydrogen in Propellant Tanks. Vol. 9 of Advances in Cryogenic Eng., K. D. Timmerhaus, ed., Plenum Press, 1964, pp. 265-272.

5. Huntley, S. C.: Temperature-Pressure-Time Relationships in a Closed Cryogenic Container. Vol. 3 of Advances in Cryogenic Eng., K. D. Timmerhaus, ed., Plenum Press, 1960, pp. 342-352.

6. Knuth, Eldon L.: Evaporations and Condensations in One-Component Systems. ARS J., vol. 32, no. 9, Sept. 1962, pp. 1424-1426.

7. Thomas, P. D.; and Morse, F. H.: Analytic Solution for the Phase Change in a Suddenly Pressurized Liquid-Vapor System. Vol. 8 of Advances in Cryogenic Eng., K. D. Timmerhaus, ed., Plenum Press, 1963, pp. 550-562.

8. Yang, Wen-Jei; Larsen, P. S.; and Clark, J. A.: Interfacial Heat and Mass Transfer in a Suddenly Pressurized Binary Liquid-Vapor System. Paper No. 64-WA/AV-1, AIAA, 1964.

9. Epstein, M.; Georgius, H. K.; and Anderson, R. E.: A Generalized Propellant Tank-Pressurization Analysis. Vol. 10 of Advances in Cryogenic Eng., K. D. Timmerhaus, ed., Plenum Press, 1965, pp. 290-302.

10. Schmidt, A.; Purcell, J. R.; Wilson, W. A.; and Smith, R. V.: An Experimental Study Concerning the Pressurization and Stratification of Liquid Hydrogen. Vol. 5 of Advances in Cryogenic Eng., K. D. Timmerhaus, ed., Plenum Press, 1960, pp. 487-497.

11. Anderson, Bernhard H.; and Kolar, Michael J.: Experimental Investigation of the Behavior of a Confined Fluid Subjected to Nonuniform Source and Wall Heating. NASA TN D-2079, 1963.

12. Bird, R. B.; Stewart, W. E.; and Lightfoot, E. N.: Transport Phenomenon. John Wiley & Sons, Inc., 1960, pp. 83; 85; 141; 319; 324.

13. Kutateladze, S. S.: Fundamentals of Heat Transfer. Second ed., R. D. Cess, ed., Academic Press, Inc., 1963.

TABLE I. - TESTS PERFORMED

[Liquid, hydrogen; liquid depth, 55 percent full or 4 ft.]

Test	Pressurant gas	Type of pressurization	Heat flux from environment, $(Q/A)_w$, Btu/(sq ft)(hr)	Nominal pressure-time conditions	Atmospheric pressure (nominal), in. Hg
1	Hydrogen	Artificial	8	$t < 0$: P'_o = 0 psig (vented);	29.25
2	Hydrogen	Artificial	8	$t \geq 0$: P' = constant	29.24
3	Helium	Artificial	8	= 8, 20, 40 psig	29.26
4	-------	Self	6.7	$t \leq 0$: P'_o = 0 (vented); $t \geq 0$: $P' = P'(t)$ up to 40 psig	28.78

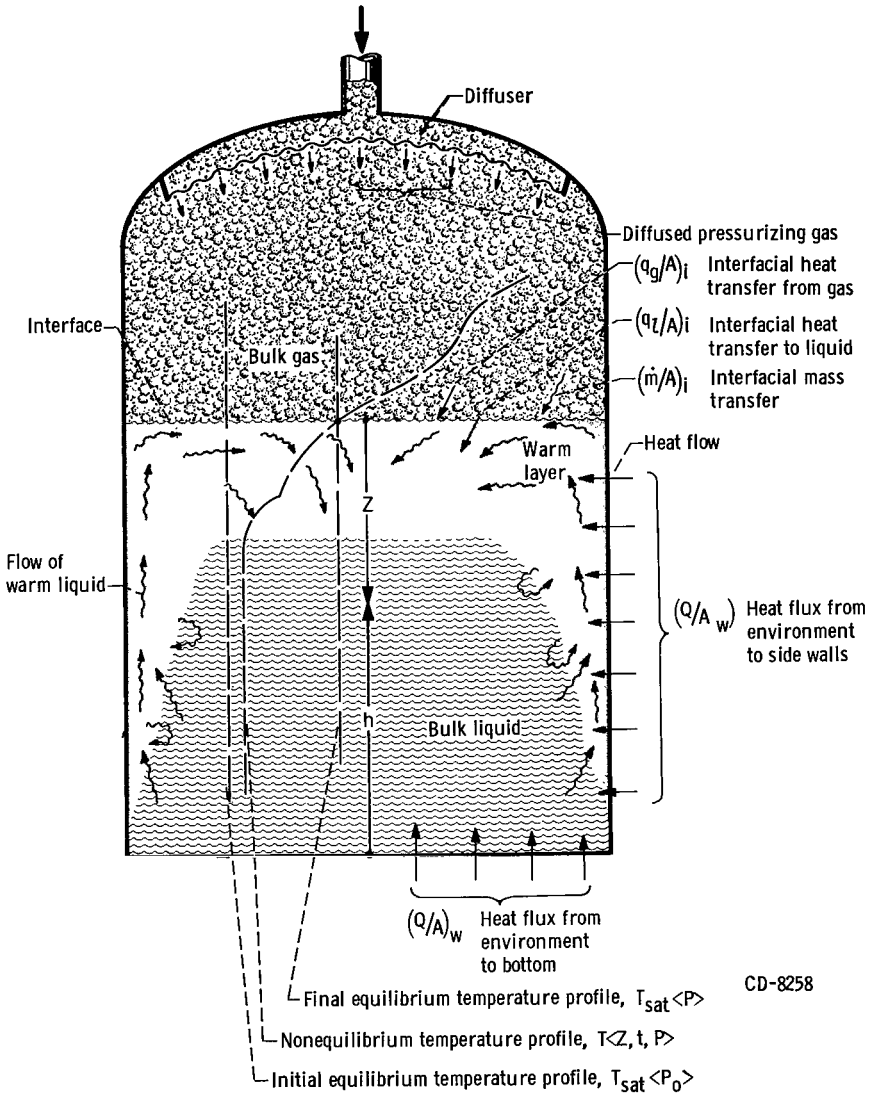

Figure 1. - Changes occuring when a tank containing a two-phase fluid is pressurized.

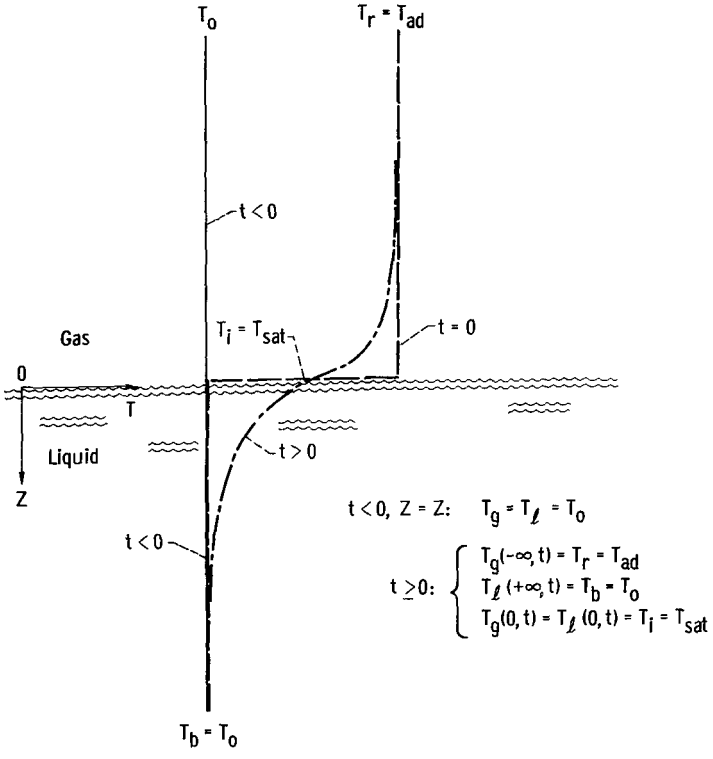

Figure 2. - Semi-infinite volume approximation to actual situation.

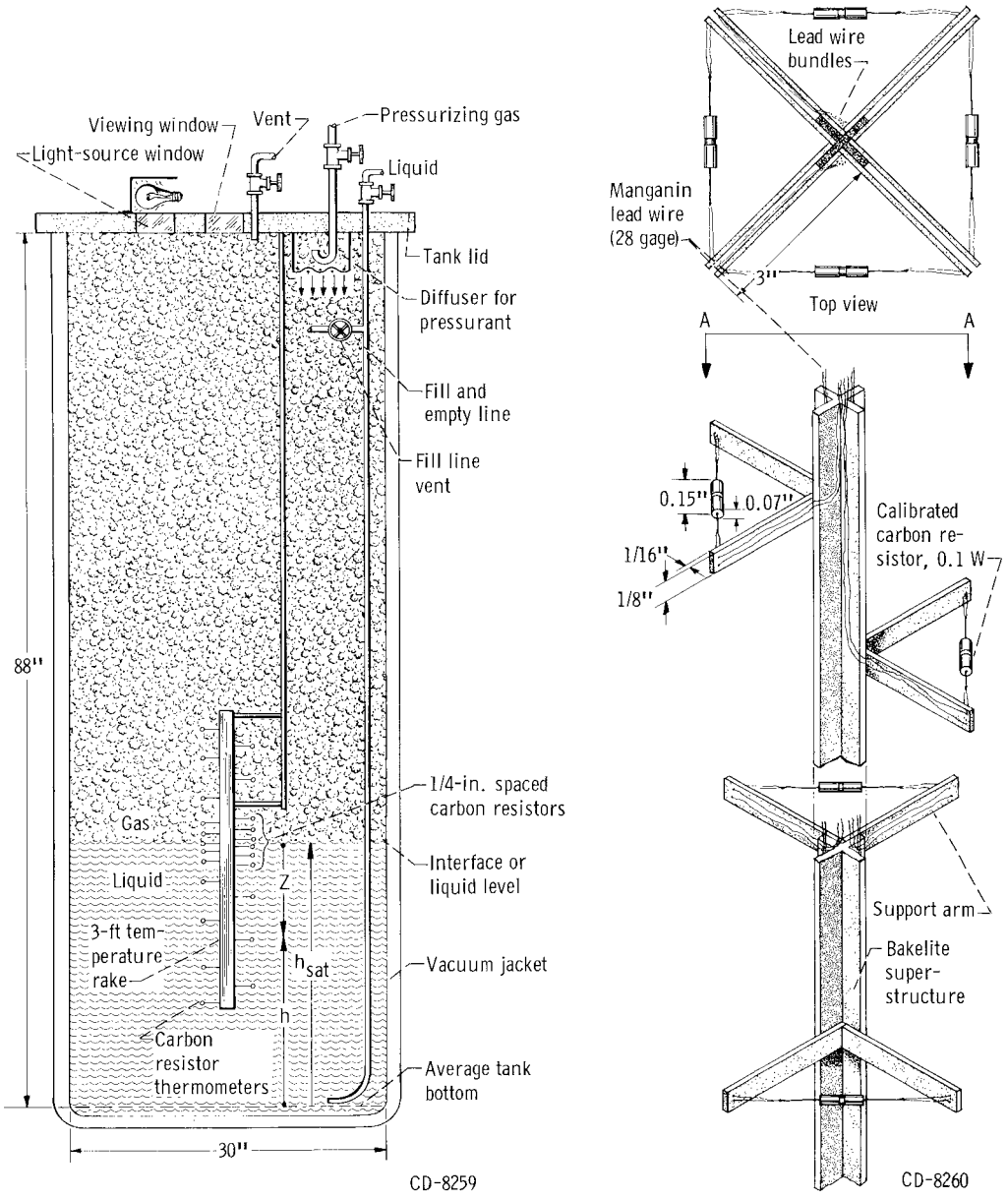

(a) Overall view.

(b) Typical section of temperature rake.

Figure 3. - Schematic of test facility for tests 1 to 4.

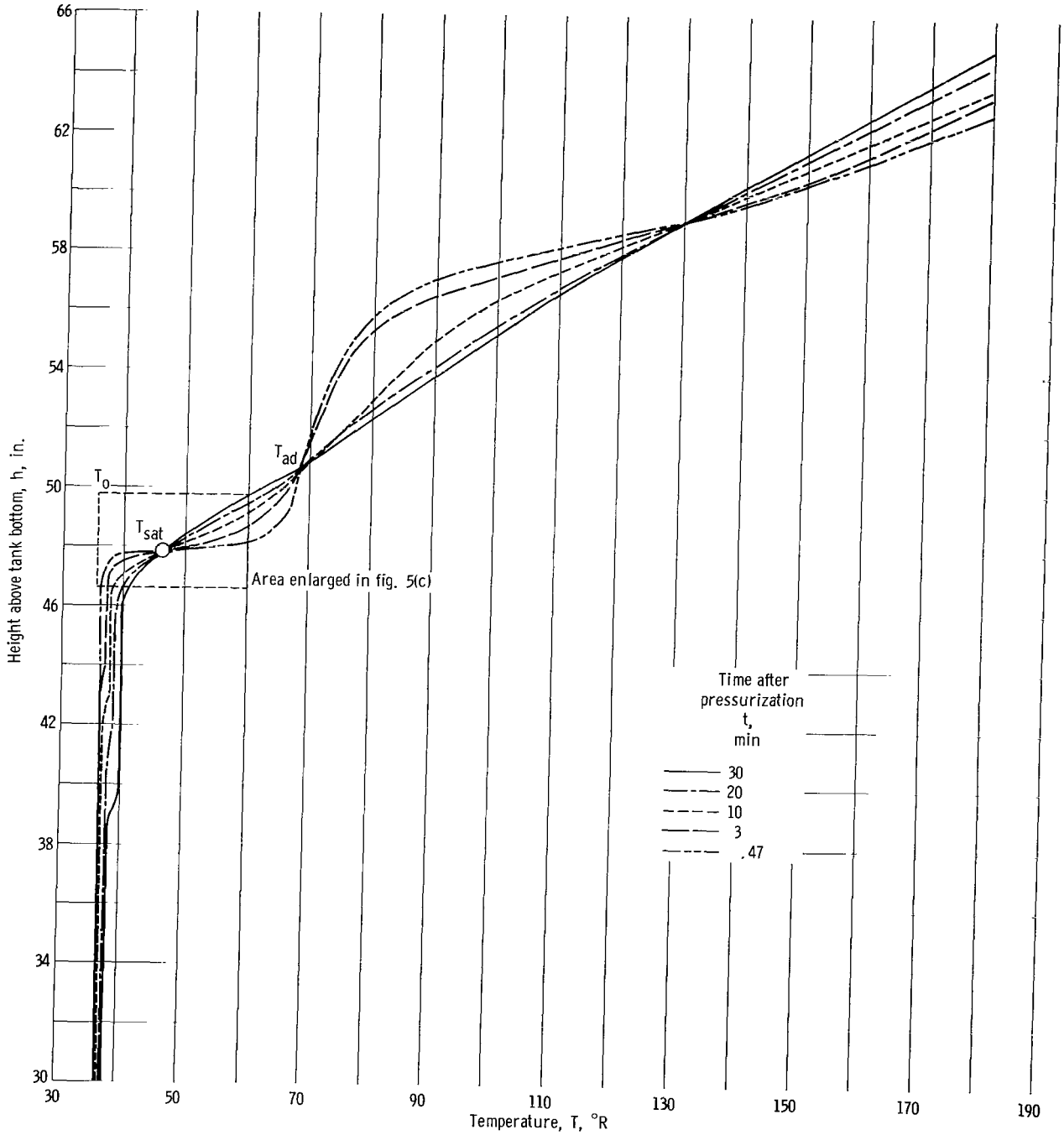

Figure 4. - Experimental temperature profile (T = T(h, t)) for test 1. Pressure, 40 pounds per square inch gage.

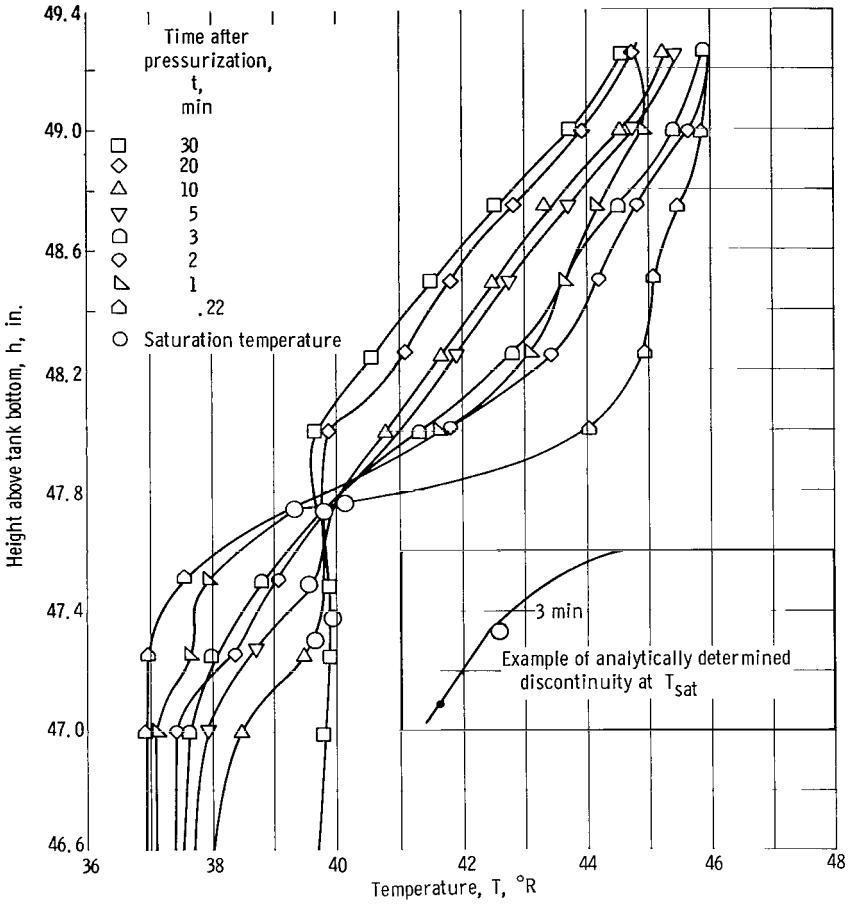

(a) Tank pressure, 8 pounds per square inch gage.

Figure 5. - Experimental temperature profile near interface for test 1.

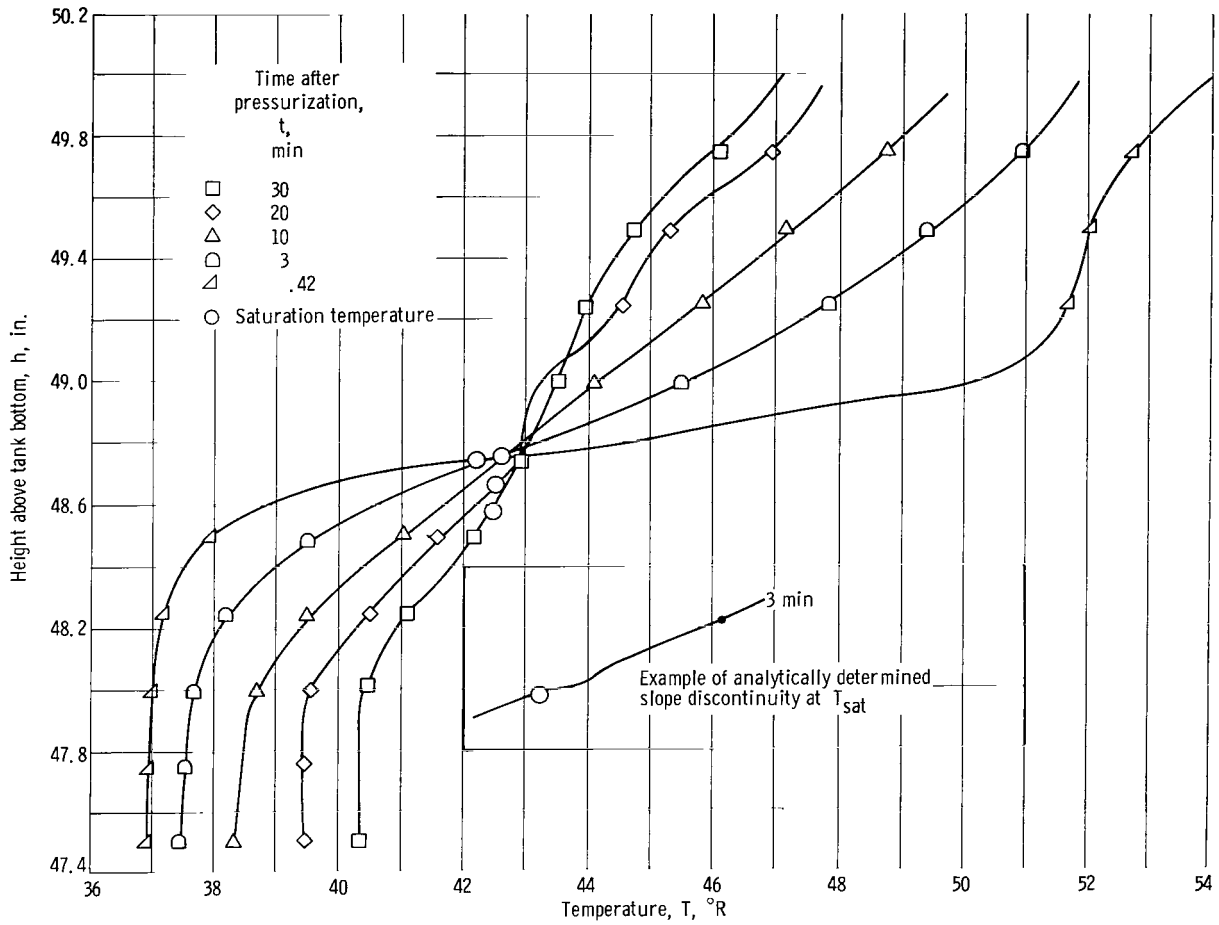

(b) Tank pressure, 20 pounds per square inch gage.

Figure 5. - Continued.

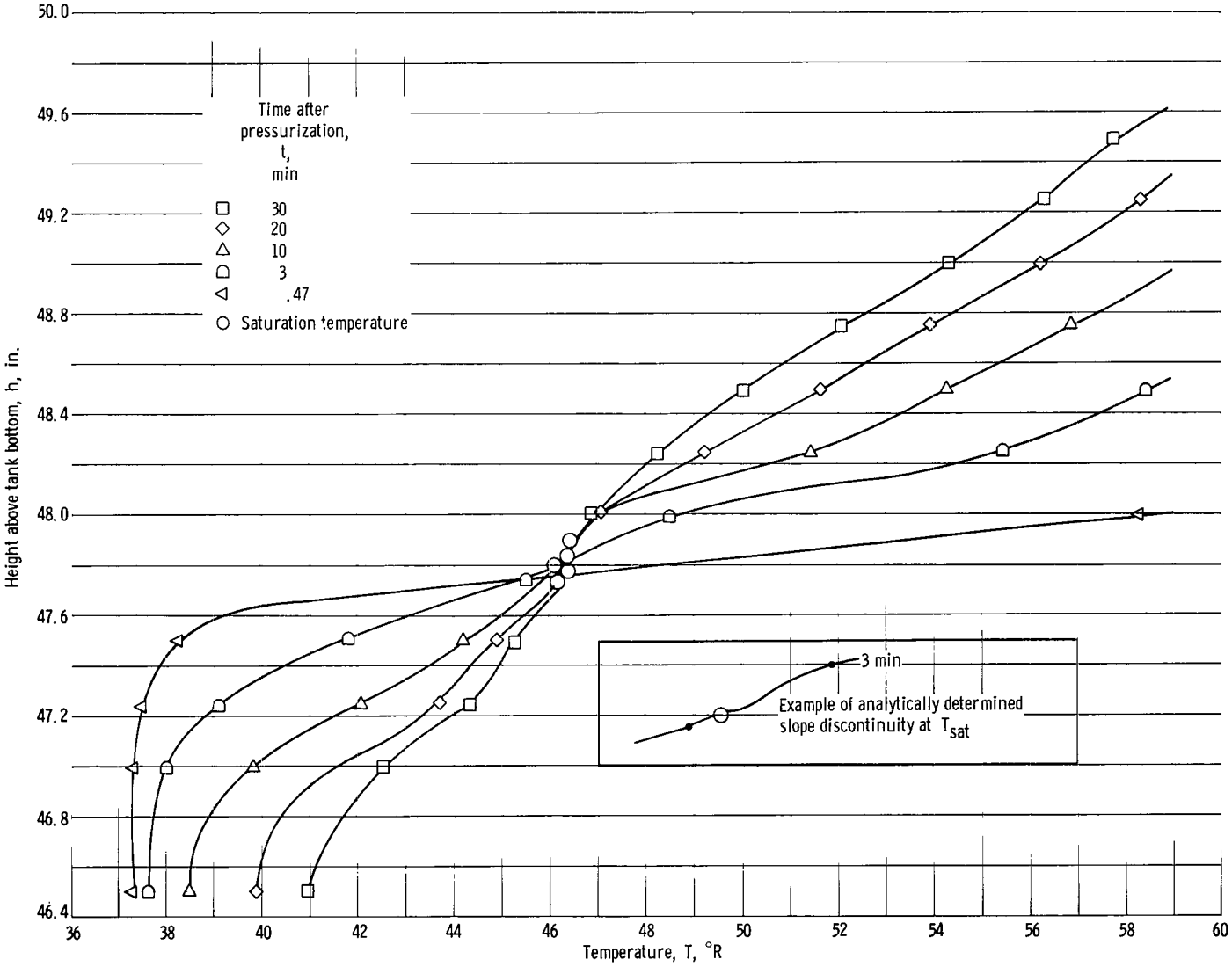

(c) Tank pressure, 40 pounds per square inch gage.

Figure 5. - Concluded.

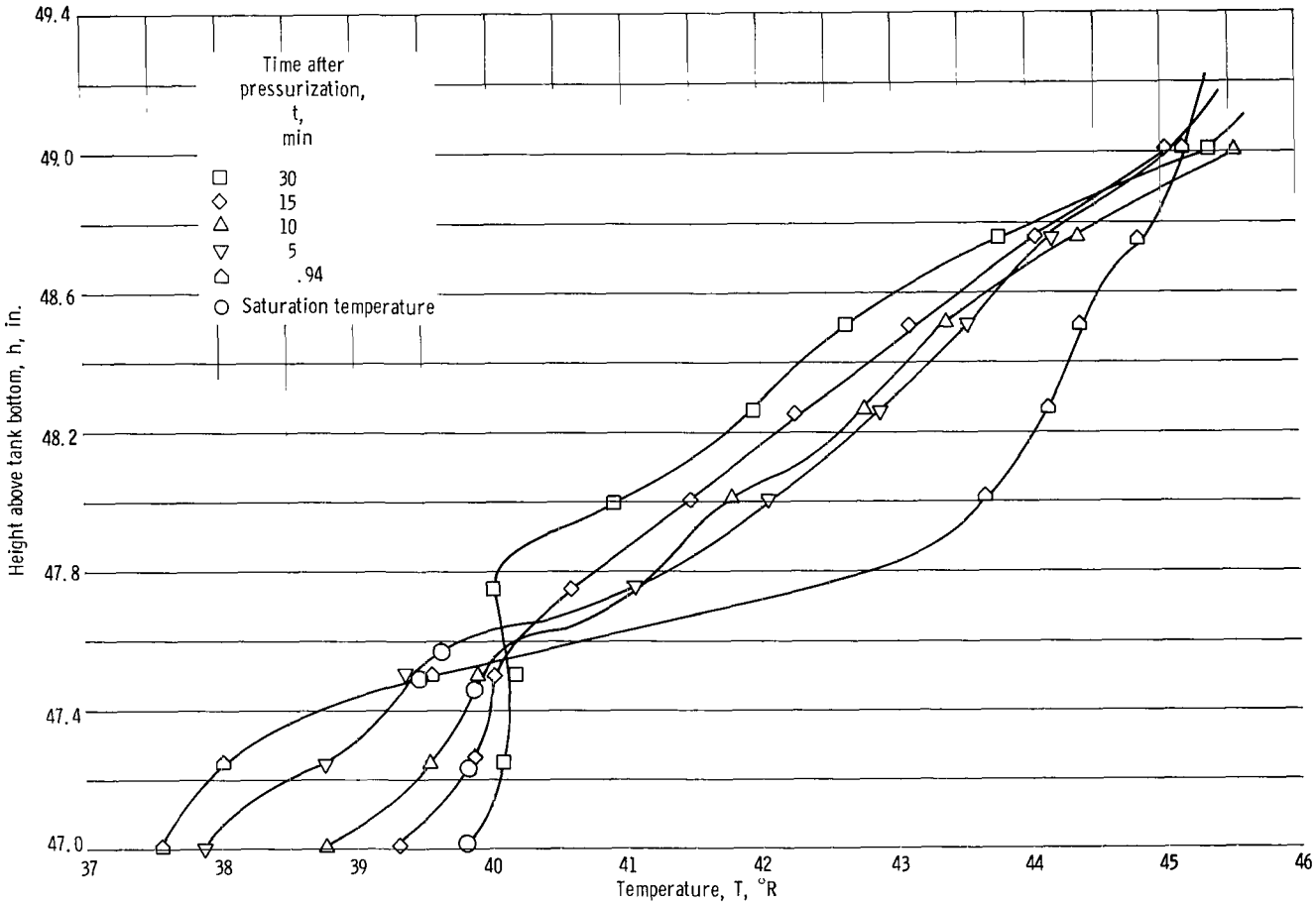

(a) Tank pressure, 8 pounds per square inch gage.

Figure 6. - Experimental temperature profiles near interface for test 2.

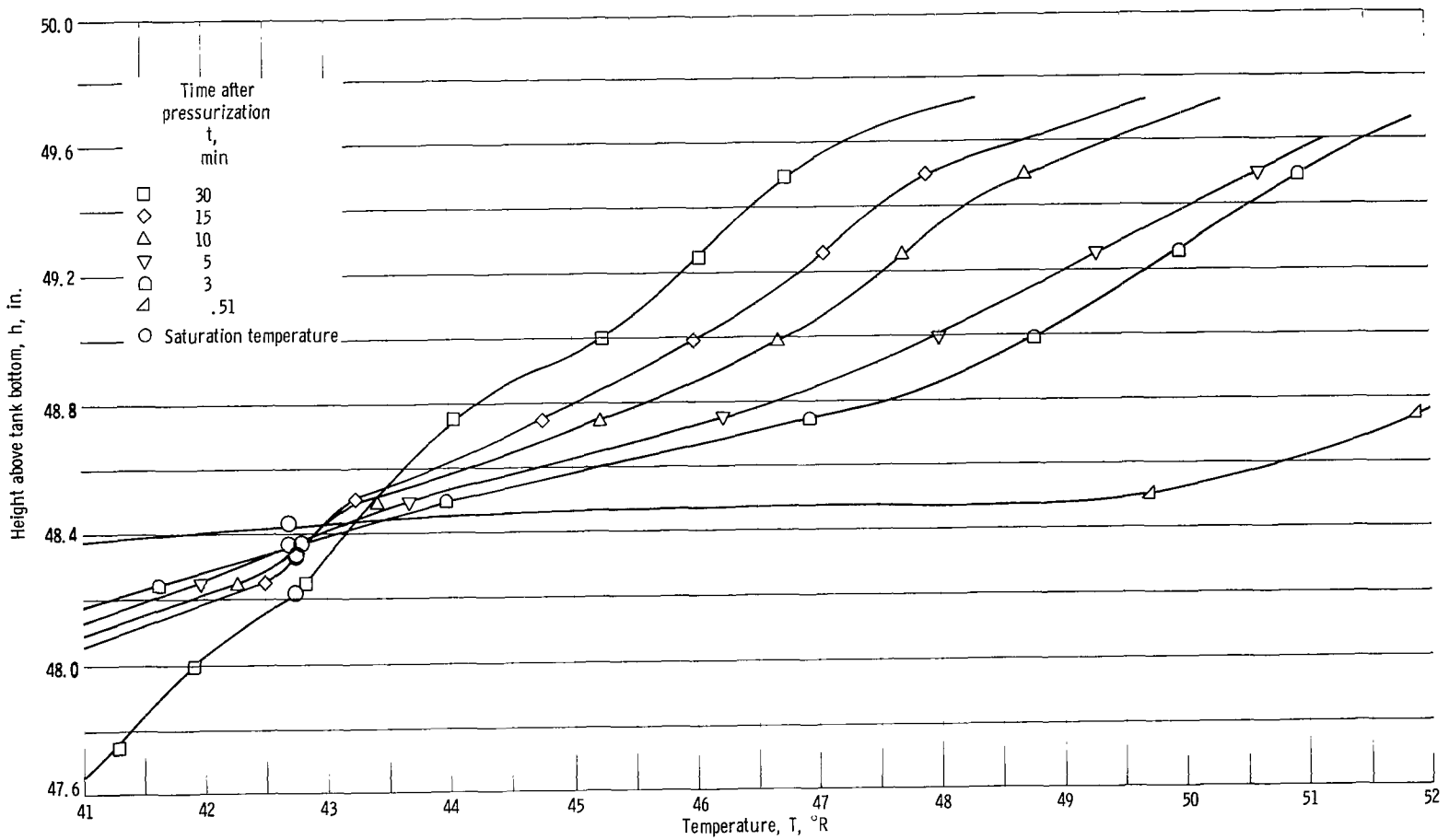

(b) Tank pressure, 20 pounds per square inch gage.

Figure 6. - Continued.

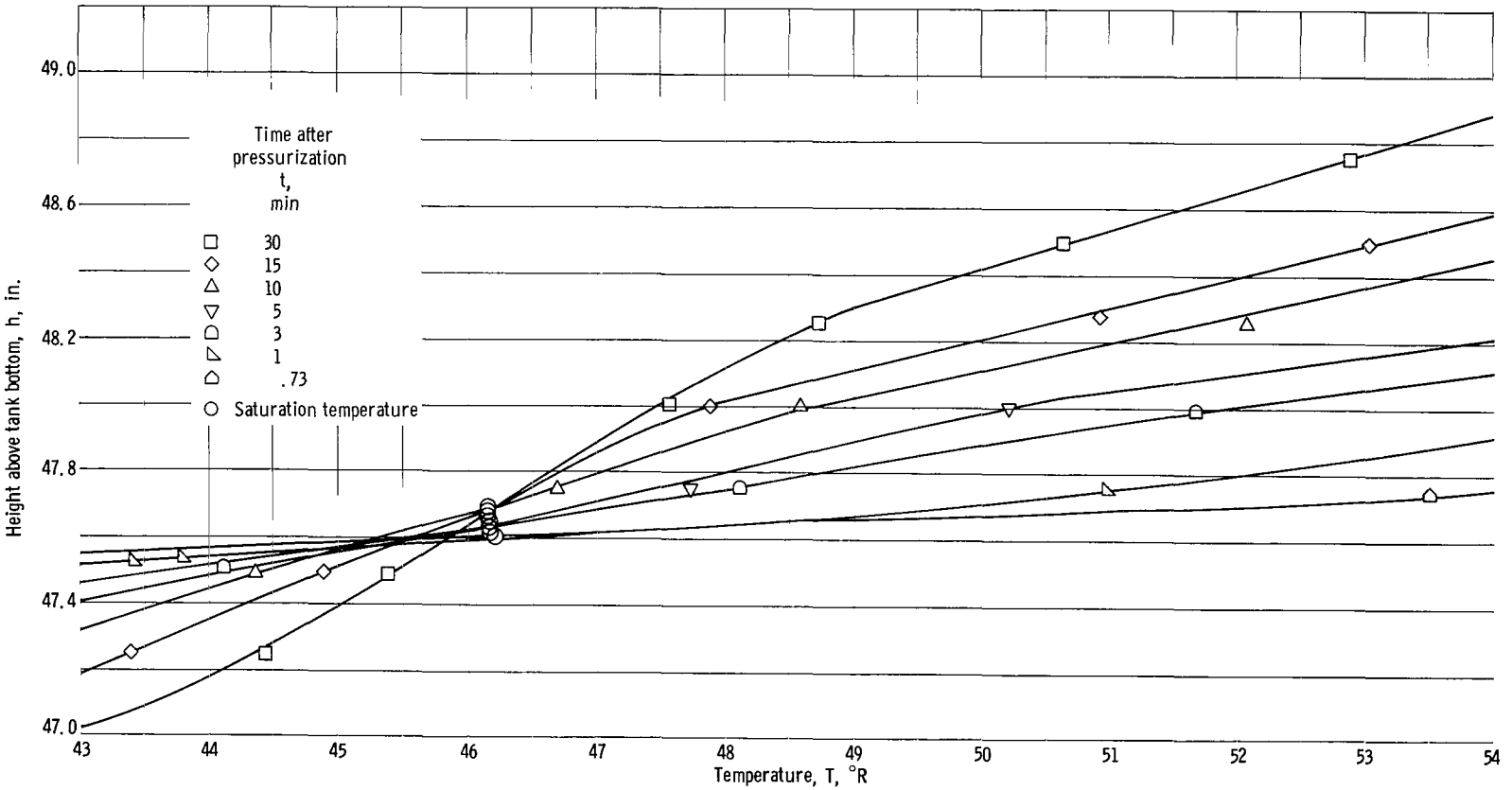

(c) Tank pressure, 40 pounds per square inch gage.

Figure 6. - Concluded.

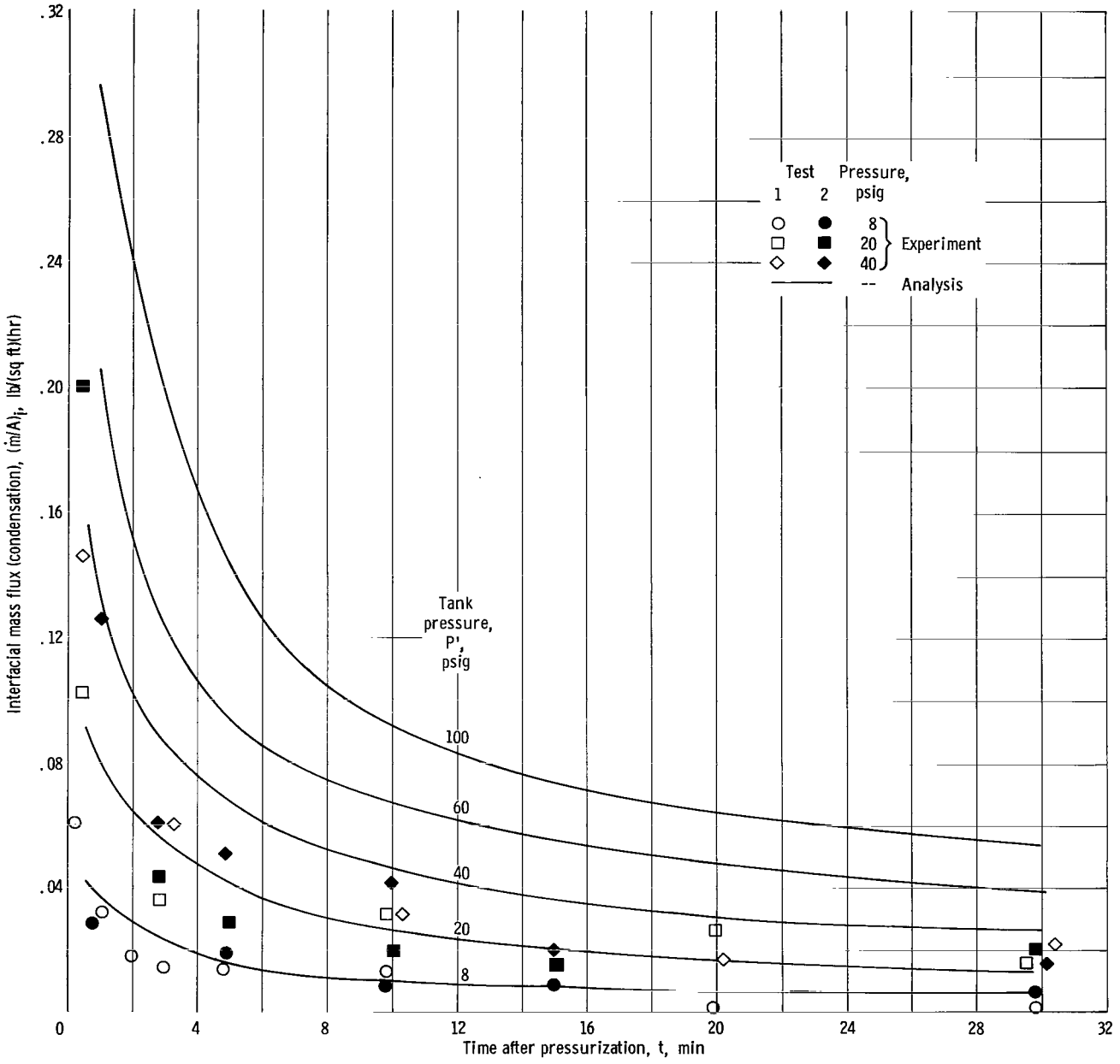

Figure 7. - Interfacial mass flux based on saturated interface at constant pressure.

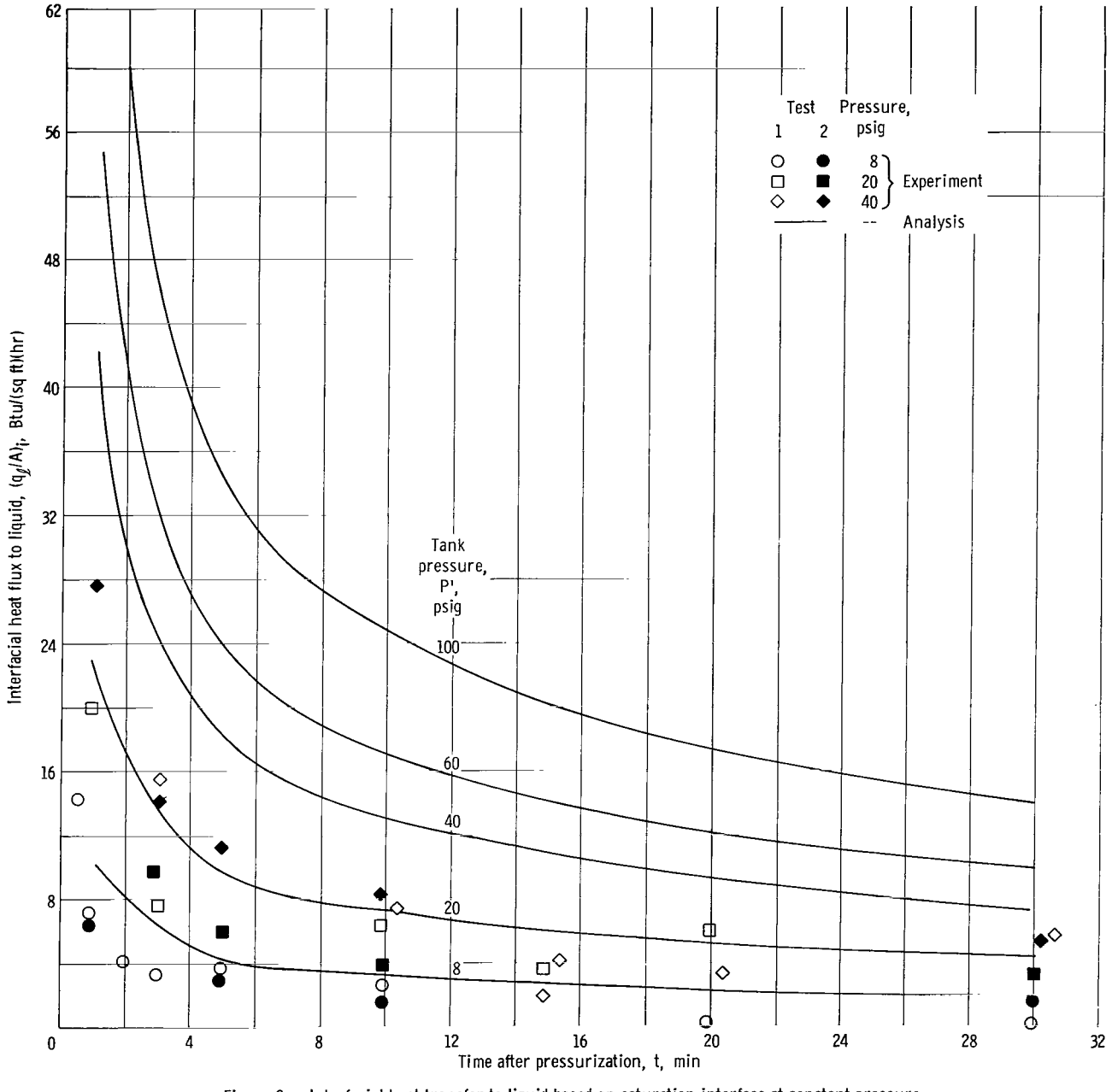

Figure 8. - Interfacial heat transfer to liquid based on saturation interface at constant pressure.

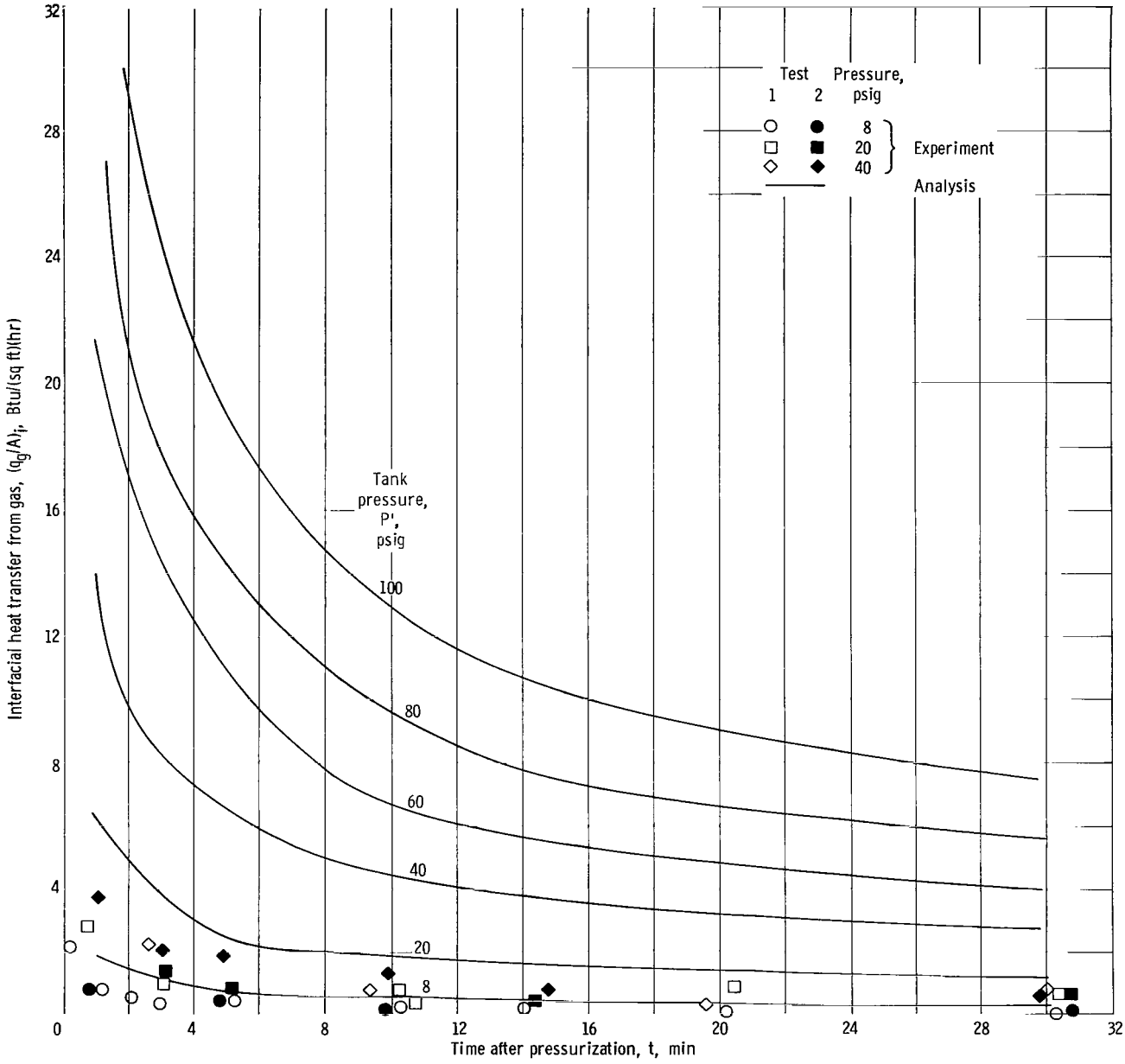

Figure 9. - Interfacial heat transfer from gas based on saturated interface.

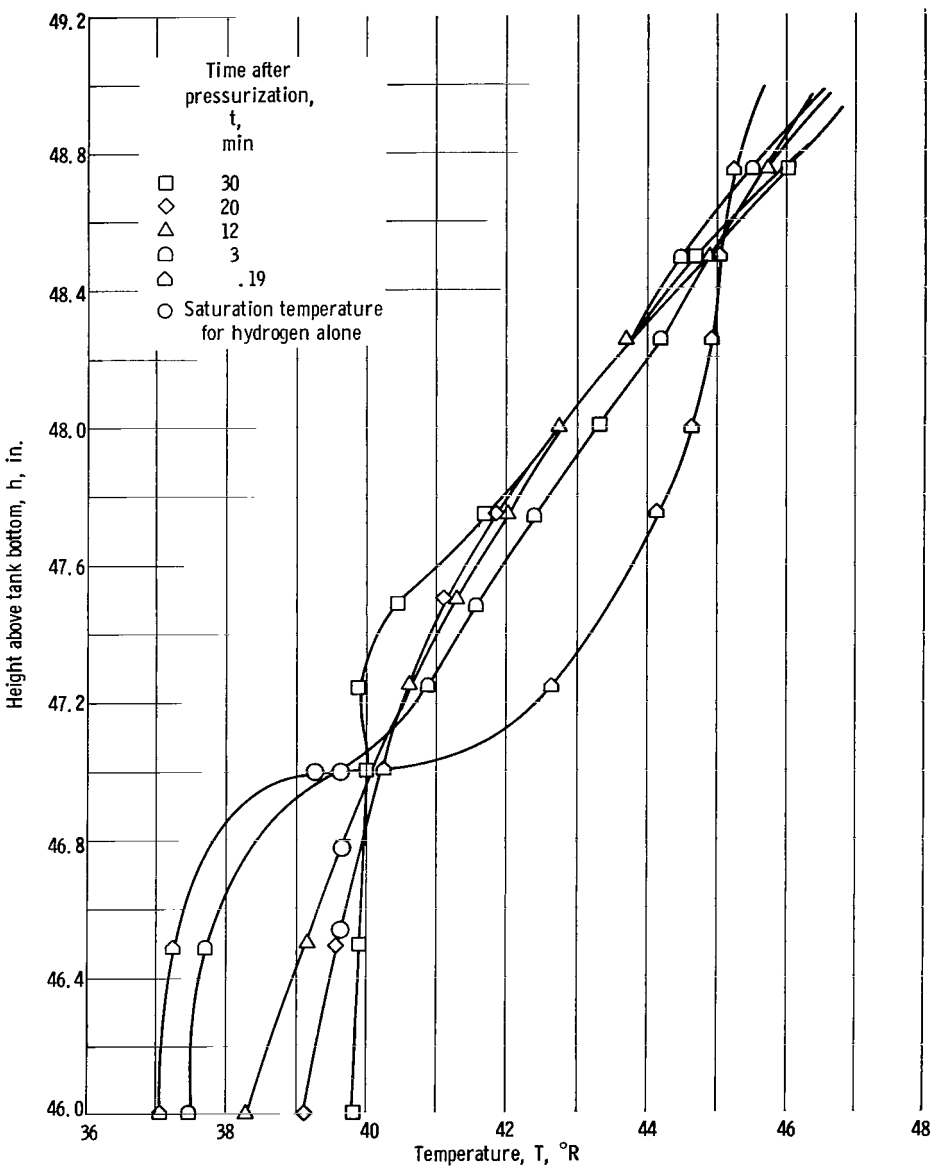

(a) Tank pressure, 8 pounds per square inch gage.

Figure 10. - Experimental temperature profiles near interface for test 3 with helium pressurant.

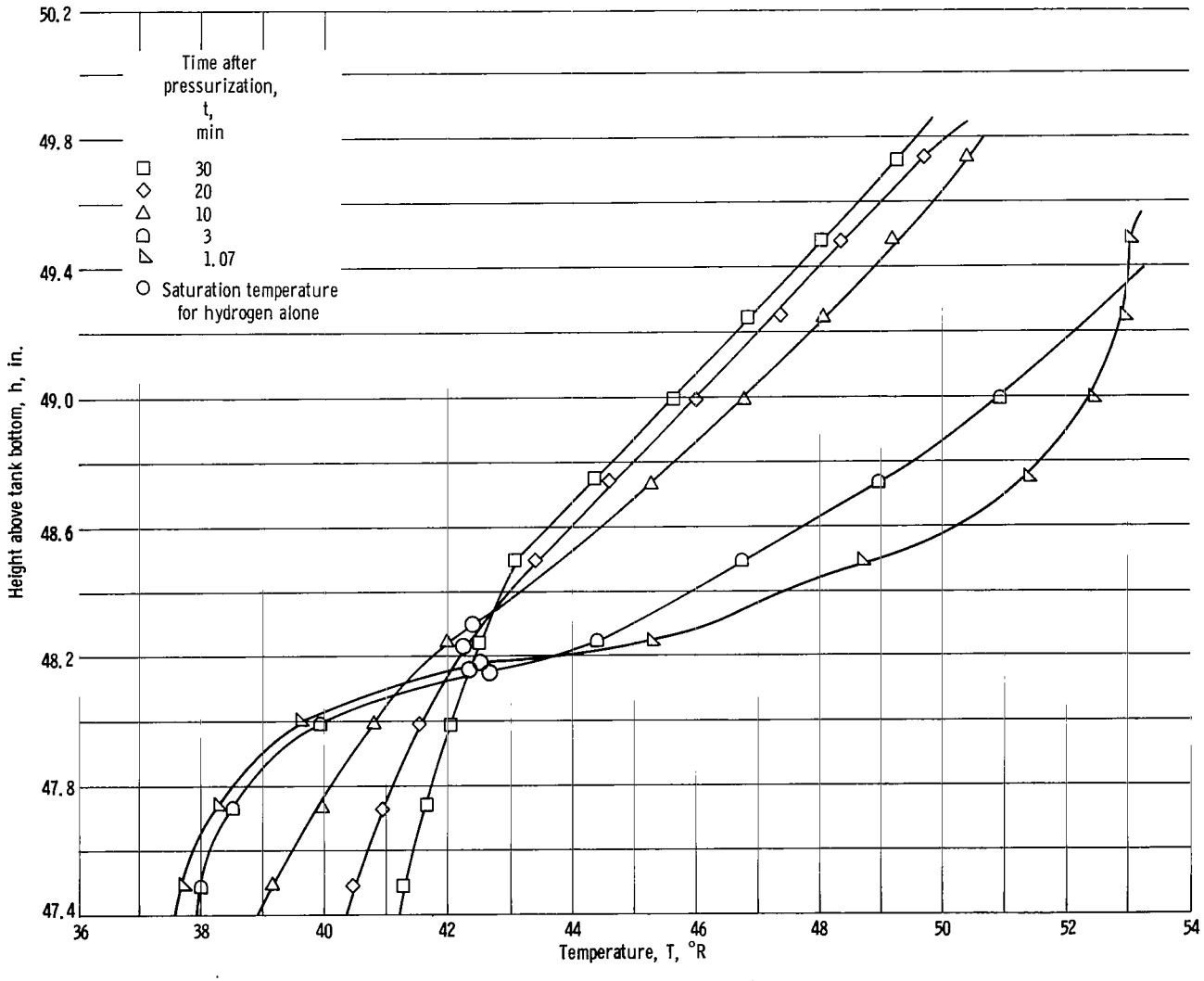

(b) Tank pressure, 20 pounds per square inch gage.

Figure 10. - Continued.

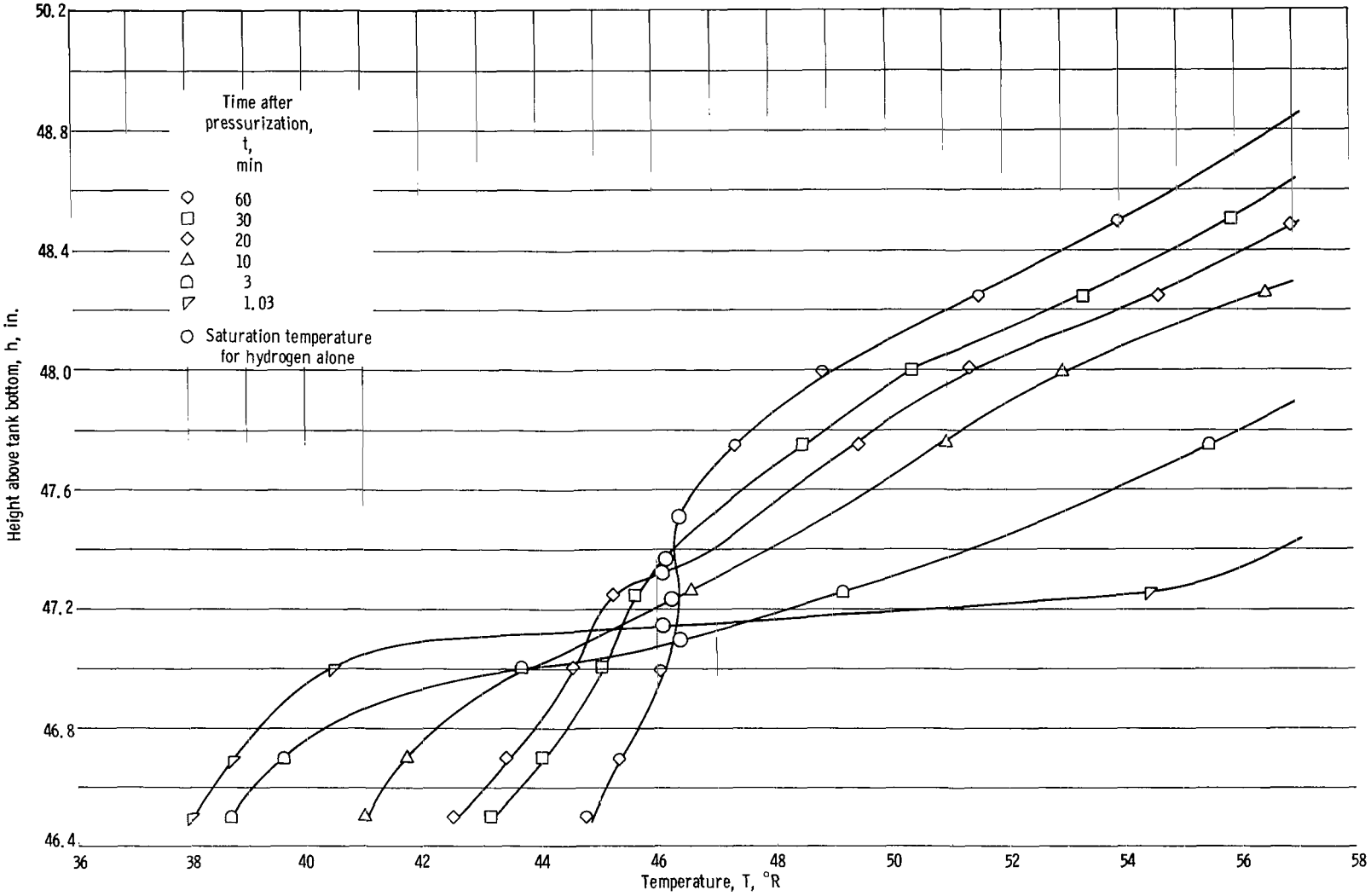

(c) Tank pressure, 40 pounds per square inch gage.

Figure 10. - Concluded.

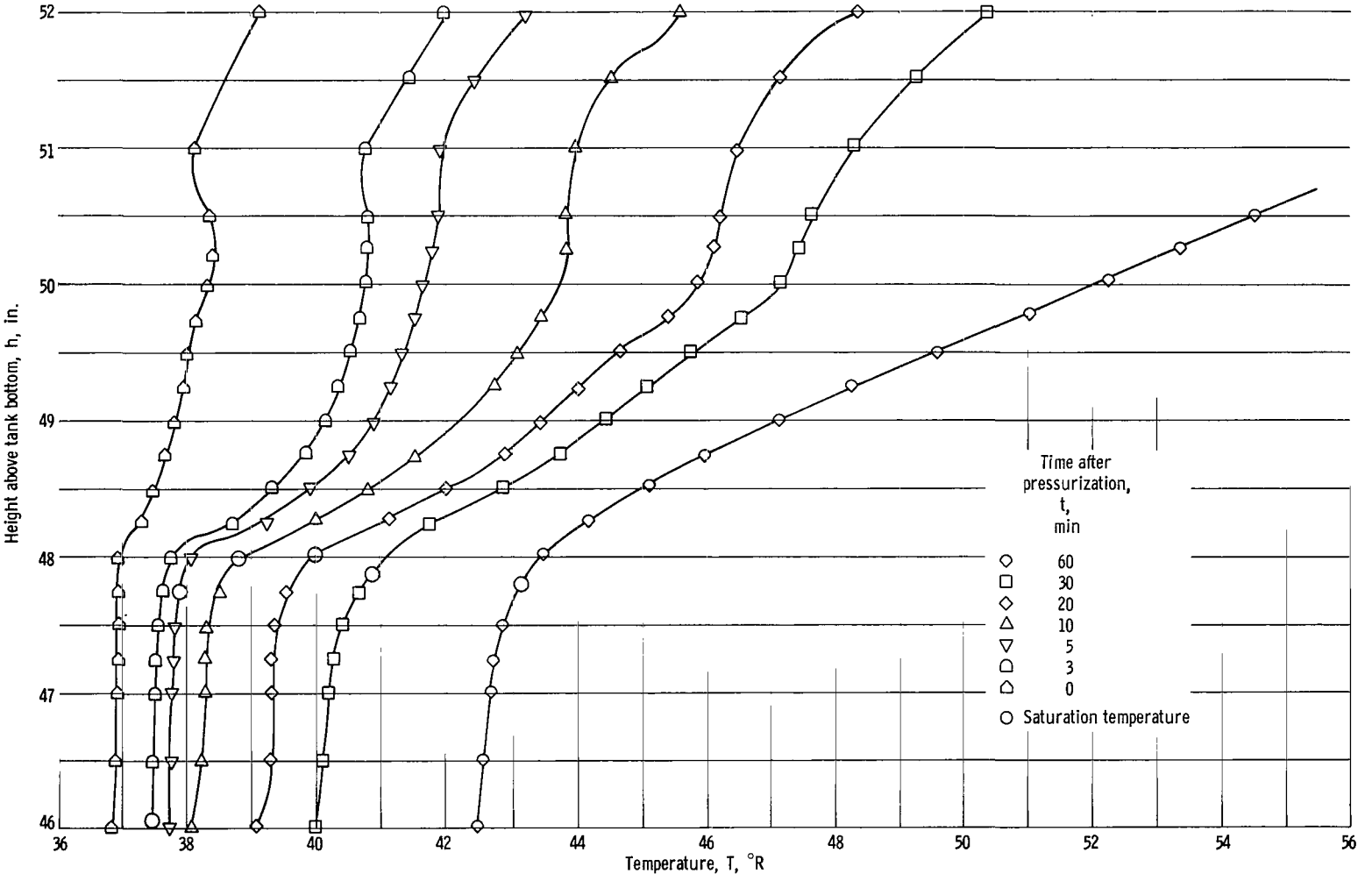

Figure 11. - Experimental temperature profiles near interface for test 4 with self-pressurization.

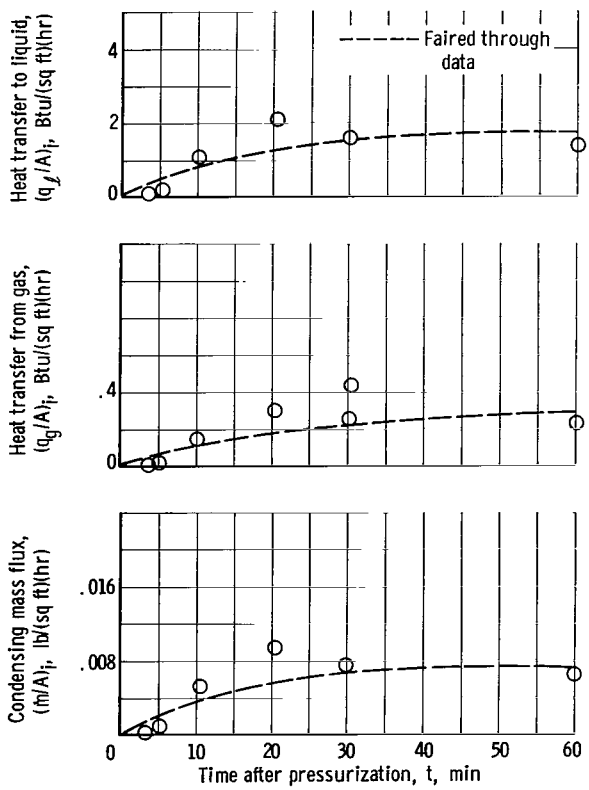

Figure 12. - Experimental interfacial fluxes for self-pressurization test (test 4).

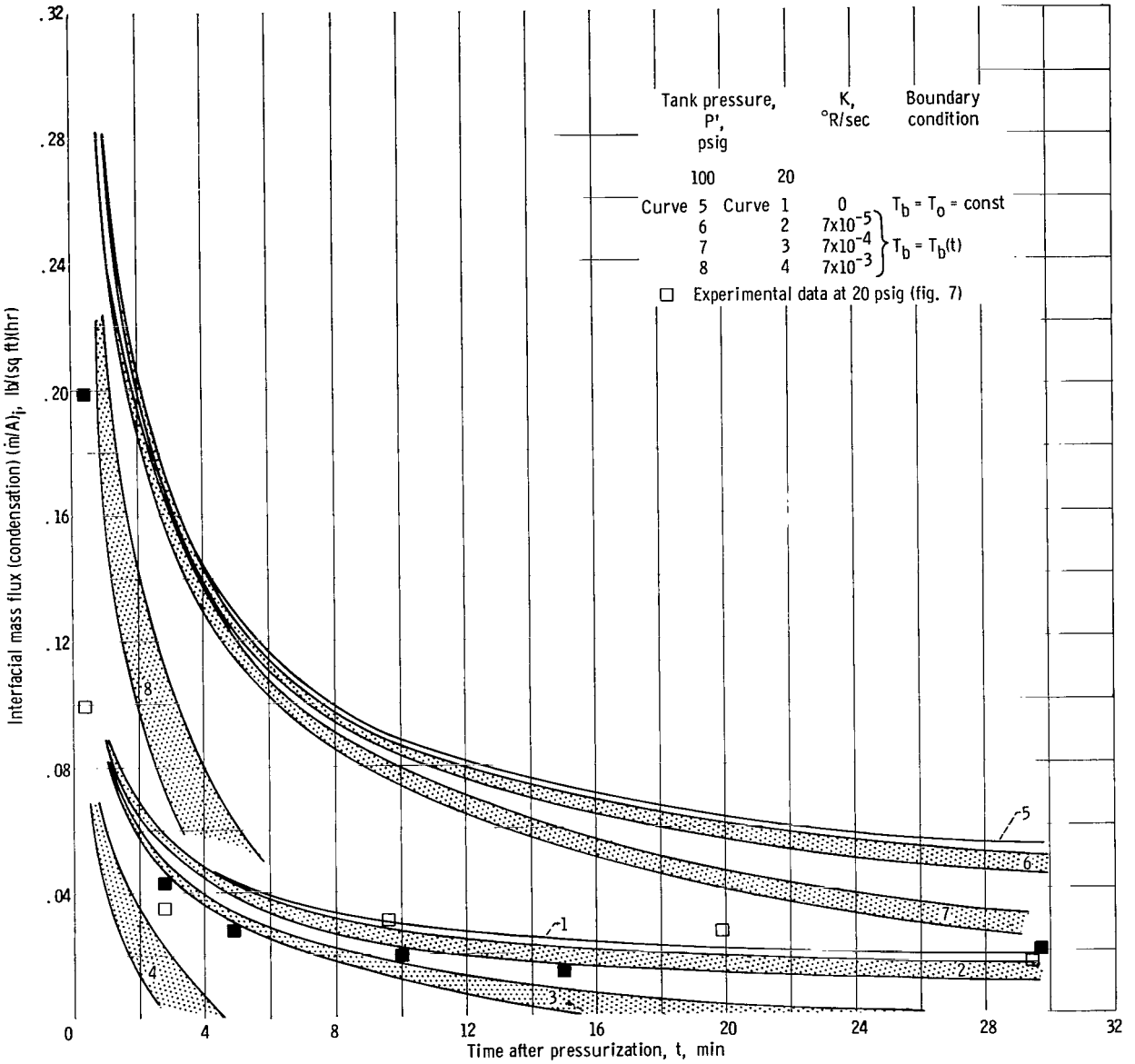

Figure 13. - Analytically determined effect of liquid heating on condensation rate. Range of liquid-depth to tank-diameter ratio, 2 to 0.5.

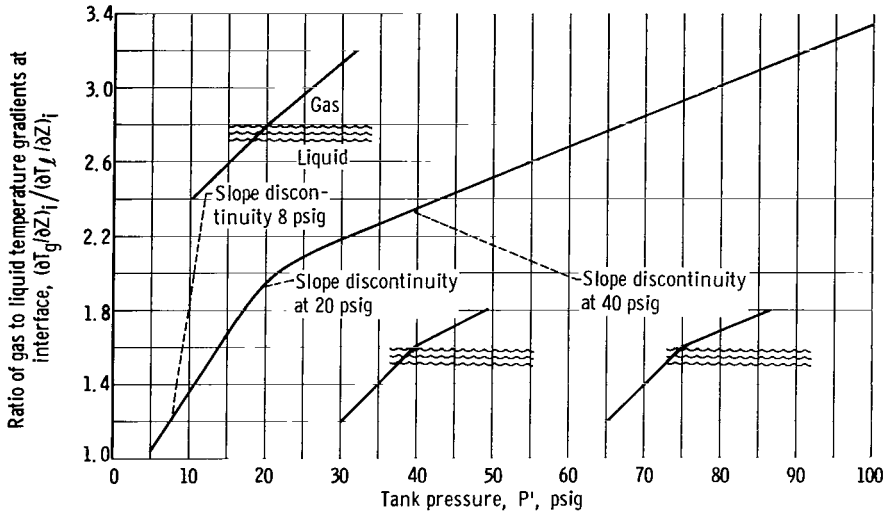

Figure 14. - Analytical slope discontinuity at saturation interface.

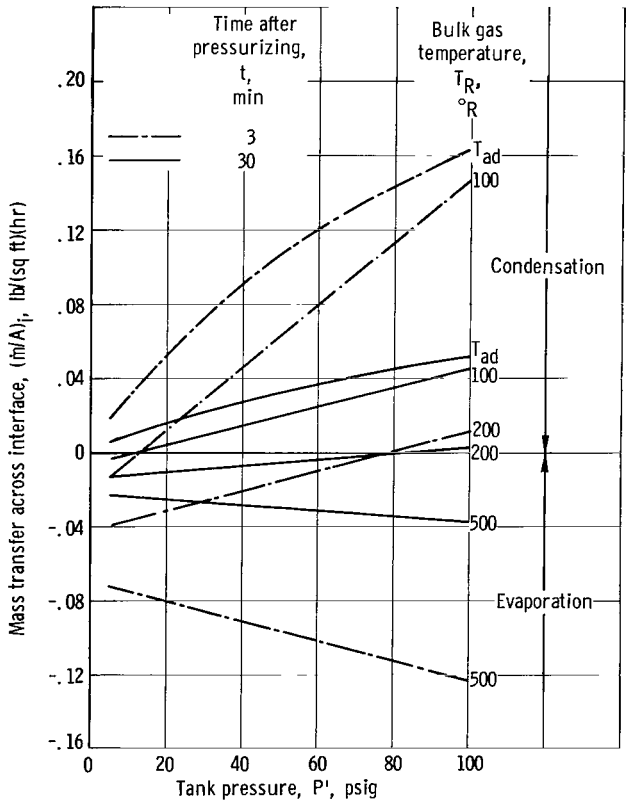

Figure 15. - Effect of bulk gas temperature on interfacial mass transfer for 3 and 30 minutes after pressurizing.

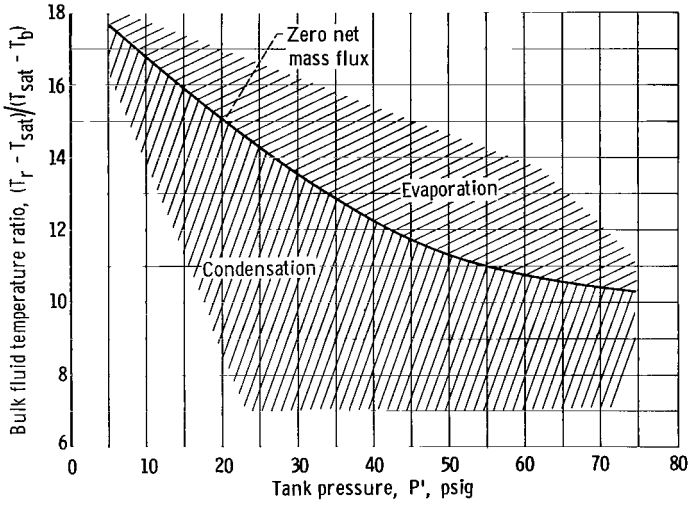

Figure 16. - Direction of mass flux as function of bulk fluid temperatures and tank pressure for hydrogen.

"The aeronautical and space activities of the United States shall be conducted so as to contribute . . . to the expansion of human knowledge of phenomena in the atmosphere and space. The Administration shall provide for the widest practicable and appropriate dissemination of information concerning its activities and the results thereof."

—NATIONAL AERONAUTICS AND SPACE ACT OF 1958

NASA SCIENTIFIC AND TECHNICAL PUBLICATIONS

TECHNICAL REPORTS: Scientific and technical information considered important, complete, and a lasting contribution to existing knowledge.

TECHNICAL NOTES: Information less broad in scope but nevertheless of importance as a contribution to existing knowledge.

TECHNICAL MEMORANDUMS: Information receiving limited distribution because of preliminary data, security classification, or other reasons.

CONTRACTOR REPORTS: Technical information generated in connection with a NASA contract or grant and released under NASA auspices.

TECHNICAL TRANSLATIONS: Information published in a foreign language considered to merit NASA distribution in English.

TECHNICAL REPRINTS: Information derived from NASA activities and initially published in the form of journal articles.

SPECIAL PUBLICATIONS: Information derived from or of value to NASA activities but not necessarily reporting the results of individual NASA-programmed scientific efforts. Publications include conference proceedings, monographs, data compilations, handbooks, sourcebooks, and special bibliographies.

Details on the availability of these publications may be obtained from:

SCIENTIFIC AND TECHNICAL INFORMATION DIVISION

NATIONAL AERONAUTICS AND SPACE ADMINISTRATION

Washington, D.C. 20546